DEVELOPMENT OF A MAGNETORHEOLOGICAL PINCHED MODE VALVE FOR AUTOMOTIVE SEMI-AUTOMOTIVE SEMI-ACTIVE SUSPENSION SYSTEM

RDU160318

Izwan Ismail

UMP Research Grant Final Report

UNIVERSITI MALAYSIA PAHANG

June 2018

ABSTRAK

Cecair Magneto-rheologi (MR) adalah salah satu bahan pintar yang sifat reologinya berubah dengan pantas kerana penggunaan medan magnet. Dalam kajian ini, reka bentuk baru injap MR pada aplikasi mod cetakan telah dicadangkan. Tujuan kajian ini untuk mengoptimumkan injap mod MR yang baru pada aplikasi rintangan pada tekanan tinggi melalui kajian mengenai parameter geometri bagi mekanisme injap. Kajian ini telah dijalankan melalui kaedah reka bentuk percubaan (DOE) dengan menggunakan model faktorial 2 peringkat. Sebaliknya, perisian Perisian Unsur Magnet (FEMM) telah digunakan untuk mensimulasikan medan magnet yang dihasilkan oleh gegelung elektromagnet dalam injap mod MR. Analisis konsep reka bentuk adalah untuk mengesahkan bidang berkesan mod cengkaman untuk julat tekanan dan kepadatan fluks yang boleh diterima. Selain itu, pada parameter mod sempit injap boleh keluar dengan mendapatkan kelikatan yang rendah dengan tekanan yang tinggi melalui komposisi bendalir MR dalam saluran bahagian yang sempit. Konvensional jurang, jurang injap dan konfigurasi gegelung telah ditetapkan untuk pelbagai saiz untuk mendapatkan pengagihan medan magnet yang terbaik dan penurunan tekanan yang diperlukan. Selain itu, sifat bahan lain seperti tegasan hasil, pemendapan dan kesan bahan ke atas suhu dan medan magnet juga di ambil kira. Penemuan kajian ini menunjukkan, apabila tekanan tinggi di kenakan, medan magnet yang terhasil jua akan meningkat. Walau bagaimanapun, hubungan ini tidak begitu ketara. Penurunan tekanan meningkat hanya 0.2% manakala medan magnet menunjukkan sehingga 0.5%. Pengoptimuman parameter geometri melalui analisis model faktorial 2-peringkat telah menghasilkan enam nilai keunikan sebanyak 0.874 pada fluks magnet maksimum 1.06 Tesla

ABSTRACT

Magneto-rheological (MR) fluid is one of smart material whose rheological properties is rapidly change due to the application of the magnetic field. In this study, the new design of MR valve on pinched mode application has been proposed. The aim of this study to optimize the new MR pinched mode valve at high pressure resistance application through investigation on the effect of geometry parameter of valve mechanism. This study has been conducted through design of experiment (DOE) methodology by using 2-level factorial model. On the other hand, Finite Element Magnetic Method (FEMM) software was utilized to simulate the magnetic field generated by electromagnetic coils in MR pinched mode valve. The analysis of design concept is to verify the effective areas of pinched mode for acceptable range of pressure drop and flux density. Moreover, the investigated on pinched mode parameter can be come out by getting low viscosity with high pressure of MR fluid composition in pinched mode channel. The annular, valve gap and coil configurations are being set for various size in order to get the best magnetic field distribution and pressure drop needed. Furthermore, other material properties such as yield stress, sedimentation and material effect towards temperature and magnetic fields are also taking into consideration. The finding of this study shows, the high pressure have been applied, the high magnetic field also being produce. However, this relationship is not much significant. The pressure drop increases only 0.2 % meanwhile magnetic field shows up to 0.5 %. Optimization of geometry parameter through 2-level factorial model analysis resulting sixteen desirability value of 0.874 at maximum magnetic flux 1.06 Tesla

TABLE OF CONTENT

LIST OF TABLES

LIST OF FIGURES

CHAPTER 1

INTRODUCTION

1.1 Introduction

Magnetorheological (MR) fluid is a functional material that rheologically responsive on magnetic field excitation. The response is rapid, with an estimated response time of less than 10ms and self-react in its environment without help from electronic actuators. The reaction resulting changes of suspended particle structure thus affecting the apparent viscosity. It also has ability to change from Newtonian liquid state into a semisolid non-Newtonian state with relatively low power consumption. They are basically three components in an MR Fluid: The carrier fluid, the magnetic particles and the stabilizing additives. The carrier fluid has the main function to carry the magnetic particle as well as naturally provides lubrication and damping features. The magnetic particles are usually made of carbonyl iron, iron oxide, or iron/cobalt alloys to achieve high magnetic saturation. While the additives, including stabilizers and surfactants, are used to improve bonding stability between the carrier fluid and the magnetic particles, to prevent settling of the particles as well as increasing the wear resistance of the fluid. The density of MR fluid is highly determined by the formulation and composition of the fluid components, but it is typically around 3-4 g/cm3.

1.2 Problem statement

Most of MR device working principles based on the manipulation of fluid flow rate, the key performance of MR device is determined by the performance of MR valve. Therefore, a successful improvement of MR valve performance can give a significant impact to the development of other MR devices. Valve mode of MR fluids functioned by choking the material flow in a small region of annular channel by means of magnetic field. The flow which is normally due to mechanical excitation produced a pressure-difference when being choked. In previous study, approach used in enhancing the performance was by improving the design of the valve itself. In valve mode, major problem that hindered the boost of performance was dealt with liquid-particle migration problem due to active self- relocation particles behaviour within magnetic field induction. Extreme migration leads to instability of redispersion rate and a "jamming" problem. Jamming is a situation where clot happened. It is a significant problem in MR valves due to irreversible effect and thus degrades the performance. Previous study suggests that "jamming" was due to the particle size distribution of MR fluid, too high enough magnetic field strength [13-14]. At critical field strength, the granular nature of the coarse-particle fluid would initiate a jam in the valve, resulted in a sudden increase of pressure. Redesign the valve mode device with newly introduced pinched mode is a possible solution without compromising the MR material properties. The difference between a conventional MR fluid valve and the pinched mode valve is in the arrangement of the magnetic circuit where, the flow channel replaced with orifice. Magnetic poles placed axially along the flow path and capable to generates a highly non-uniform magnetic field. Effective orifice diameter can be controlled continuously with the changes of magnetic field. Controlling the flow of MR fluid through a strong magnetic field gradient allow selective solidification area. Despite that, pinched mode has its own problem where the design of magnetic circuit needs to be optimised for performance and size. Tackling those problems allow new MR valve with pinched mode to be operated in very high pressure drop environment.

As to achieve a strong magnetic field gradient in pinched mode valve, electromagnetic field distribution will be modeled by using FEMM software. Through this finite element analysis, effective orifice diameter can be determined and controlled by the required magnetic field strength. The design of magnetic circuit will be the key to this modelling. In this study, a prototype of the valve developed with specific attention given to the geometrical properties of the pinched mode valve. This will involve fabrication of parts, product assemblies and finally measurement and evaluation of the pinched mode valve performance.

1.3 Research objectives.

i) To model the electromagnetic field distribution of the pinched mode valve

ii) To develop a prototype of the pinched mode valve with optimized geometrical properties

iii) To evaluate the performance of the pinched mode valve through experimental works

1.4 Scope of the research

i. Develop a concept design of the pinch mode valve.
ii. Develop a full factorial design of experiment to optimize the geometrical properties of the pinch mode valve.
iii. Simulate the magnetic field distribution of the pinched mode valve under various geometrical parameters.
iv. Fabricate the prototype of the pinch mode valve.
v. Test the magnetic field distribution of the pinch mode valve.
vi. Design an experiment based on one factor at a time (OFAT) to investigate the effect of magnetic field on the pressure drop of magneto-rheological fluid.
vii. Conduct the pressure drop test.

CHAPTER 2

LITERATURE REVIEW

2.1 Magnetorheological materials

The magnetorheological fluid is a fluid with rheological properties. The rheological properties of MR fluids can be controlled depending on the existence of magnetic fields. MR fluids will show it rheological characteristics that are non-homogenous suspensions when the absence of magnetic fields. (Horak, Sapiński, & Szczęch, 2017). MR fluids have the ability to change from a free-flowing liquid state to a solid state with restricted fluid movement when exposed to the magnetic field.(Yazid, Mazlan, Kikuchi, Zamzuri, & Imaduddin, 2014) An MR fluids contain of a high density of magnetic particles, which are typically micrometer scale that can exhibit changes in rheological properties as cited in (Hu, Long, Yu, & Li, 2014), (Dohmen, Borin, & Zubarev, 2017). The carbonyl iron particles or any other magnetic material of MR fluid are the dispersion of micron-sized (1 to 10μm).(Mahmoud, Abd, & Ghany, 1949), (Vékás, 2008)

When magnetic fields are applied, the magnetic particles inside the carrier fluid will align increasing the fluid viscosity which solid-like state. This effect reversible, this is because once magnetic field disappears the magnetic particles will back to normal condition and viscosity will return to normal as well. Figure 2.1 shows the behaviour of MR fluids. The magnetic particles which tiny carbonyls iron are floating freely when no magnetic field is applied. When magnetic fields are applied to this MR fluids, the tiny carbonyls iron will start to line up to form the chain. This condition will make the MR fluid become the solid-like state.

Magnetic particles will form a structure chain-like under a presence of magnetic fields, under this condition shear stress will produce. Shear stress of MR fluids does not depend on the magnetic fields only, but it also depends on the volume fraction of particles and particles sizes. According to (Sarkar & Hirani, 2015), with increase in volume fraction of iron particles, the MR fluids synthesized using “mixed sized particles” show better shear stress compared to the MR fluids consist of “smaller sized spherical shaped particles” and “larger sized flaked shaped particles” at the higher shear rate.

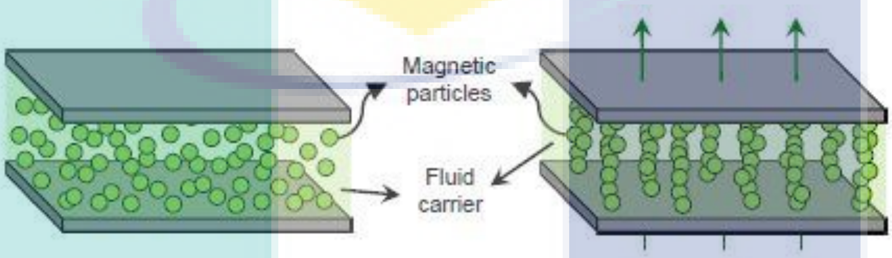

(a) (b)

Figure 2.1: The behavior of MR fluid (a) absence of magnetic field (b) presence of magnetic field

Source: (Daniel et al., 2014)

2.2 Magnetorheological valves

There are various operating modes of MR fluids devices as depicted in Figure 2.2. Figure 2.2 (a) the shear modes, (b) the flow modes, (c) the squieeze mode and (d) the pinch mode. To date, operating modes that used in magnetorheological valve are flow mode as reported in (Khan, Suresh, & SeethaRamaiah, 2014), squeeze mode as in (Saiful Amri Mazlan, 2008) and (S. A. Mazlan, Issa, Chowdhury, & Olabi, 2009), shear mode as in (Jang, Min, & Seok, 2011) and the new one is pinch mode and it also called magnetic gradient pinch (F D Goncalves & Carlson, 2009). Essentially, in all cases, MR fluids is situated between two plates yet subject to various working conditions.

For the flow mode or as known as Poiseusille flow, the MR fluids will flow between two specific plates, pressure and the resistance of flow can be control by a magnetic field. This type of operating mode can be found in devices such as MR damper. The advantages of flow mode are it can produce large damping force.

Besides, in squeeze mode, it will work when force is employed to the plates in the same manner of the direction of a magnetic field and either push toward each other or move aside from each other.(Yazid et al., 2014). The advantage of squeeze mode is, a device can achieve high damping force generated from the MR effect but this type of mode can effectively work only in a very small vibration area.

In the shear mode, the MR fluids are found between two same plates and sheared parallel to the plate that slides or then again pivots with respect to the next plate. Another point in shear mode is, solidification state at high field intensity can be avoided in MR damper, but the damping force generated from MR effect is quite small if compare with other modes.

Meanwhile, in pinch mode, The Magnetorheological Gradian Pinched (MGP) mode is a ceaseless factor control mode in which the utilization of an attractive magnetic field changes the viable measurement of the MGP orifice. Figure 2.2 illustrates how actually the arrangement of the poles of each working modes. In Figure 2.2 also, it shows where the flow gap and the path of the MR fluids are and the figure also shows, the pole of the plates which is North and South and the force acting on the plates.

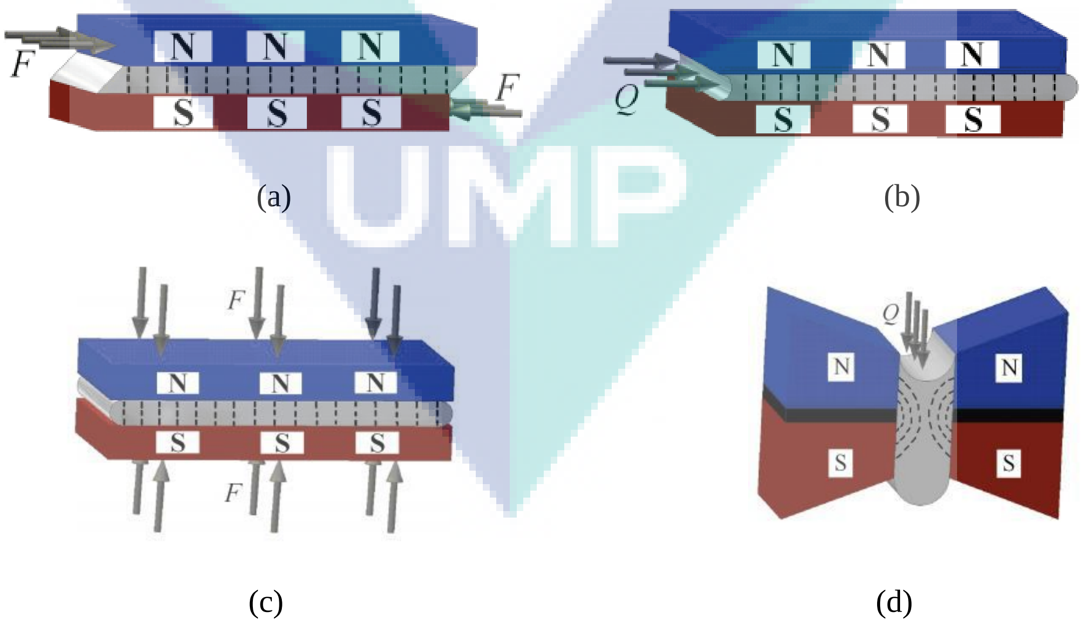

Figure 2.2: MR fluids operating mode. (a) Shear mode (b) Flow mode (c) Squeeze mode and (d) Pinch mode (Rosiakowski & Sedziak, 2012)

Generally, the MR valve used flow mode widely in the design. Motion of piston and pushes the fluid through the valves located on the piston or between the inner and outer cylinder (Wang 2011). MR fluid also flows directly between static pole pieces in valve mode. The magnetic field is applied perpendicular to the direction flow. The two fixed plates or a duct is created by a pressure drop while the magnetic field functions as a changer of rheological properties of the MR fluid in order to control the flow. Therefore, the increase in yield stress or viscosity alters the velocity profile of the fluid in the gap between two plates(Choi 2012) as per figure 2.3.

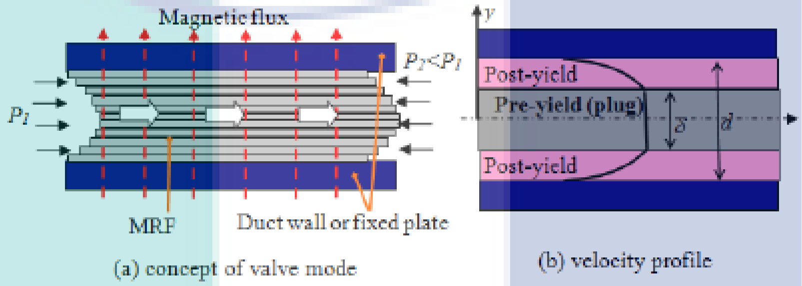

Figure 2.3 Valve mode in MR fluid application

Source: (Choi 2012)

Where,

δ = pre yield or plug region thickness
d = post yield thickness

Pressure drop ($\Delta P = P_2 - P_1$) and the flow resistance can be controlled by the magnetic field which runs normal to the flow direction (valve application) (Boelter and Janocha 1997). The value of pressure drop is defined by using the following approximation:

$$\Delta P = \Delta P_r + \Delta P_{mr} = \frac{[12 .\eta.Q.L]}{[w.g^3]} + \frac{[f.\tau_{mr}.L]}{g} \qquad 1$$

Where;

P_r = Purely Rheological

P_{mr} = Magneto-rheological Pressure Drop

τ_{mr} = Yield Stress (respond to the applied magnetic field)

Q = Flow Rate (m^3/s)

L, w, g = Geometric Length, Width and Gap size of the flow channel (m)

Based on the Equation 1 above, the purely rheological *Pr* term is valid for rectangular ducts. The magneto-rheological pressure drop P_{mr} is dependent on applied magnetic field. The magnetic field dependent component is the yield stress, τ_{mr}, which is developed in response to the applied magnetic field. The relationship between the purely rheological and the magneto rheological part in the Equation 1 is complex. Therefore an empirical factor,*f* - (no units) has been introduced.

In the case where the magneto-rheological part is more significant, i.e. *Pmr/ Pr* is about 100, this factor is 3. When the fluid movement is large, purely rheological component of Equation 1 is most important in determining the pressure drop, and *f* - must be reduced to the lower value (2 or less). The pressure drop in the rectangular channel caused by fluid flow Q [m³/s] through the gap g [mm] with particular dynamic viscosity η [Pa.s] is defined with the following equation:

$$\Delta p = \frac{12\,.\eta.L.Q}{w\,.g^3} \qquad 2$$

By using Equation 2, the purely rheological pressure drop in the valve can be calculated.

In previous study, valve mode has been said was widely used in the damper and shock absorbers and has vast application in automobile industry (Deepak Baranwal1 December 2012). In damper, valve mode applications generally consist of a cylinder and a piston. In valve mode, when MR fluid is exposed to magnetic flux lines, the areas are it's usually referred to as "choking points" (see illustrations in Figure 2.4).

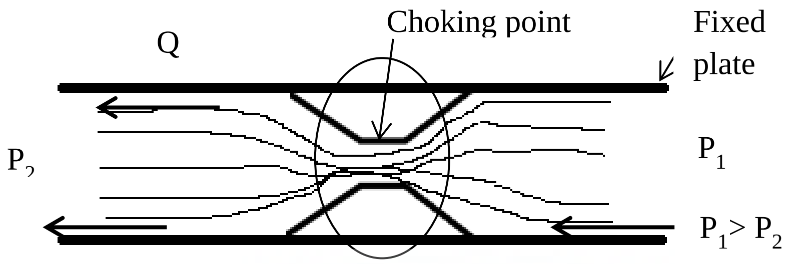

Figure 2.4 Choking point of Valve mode

Where;

Q = Air mass flow rate

P_1 = Inlet pressure

P_2 = Outlet pressure

In the case of the damper depicted in Figure 2.2, MR fluid restricts the flow of fluid from one side of the piston to the other when the fluid is in the vicinity of the “choking points” shown. The flow resistance and thus the pressure drop $\Delta P = P_1 - P_2$ can be controlled by the magnetic field which runs normal to the flow direction (Boelter and Janocha 1997). Varying the magnetic field strength, it has an effect of changing the apparent viscosity of the MR fluid. The phrase “apparent viscosity” is used since the carrier fluid exhibits no change in viscosity as the magnetic field strength is varied. Upon exposure to a magnetic field, the MR fluid as (a whole) will appear to have undergone a change in viscosity. As the magnetic field strength increases, the resistance to fluid flow at the choking point’s increases until the saturation point has been reached. In particular, the function of air flow shows the saturation behaviour of $P_2/P_1 \leq P_{critical}$ corresponding to choke flow.

Based on previous study, the factors that give affects in increasing of apparent viscosity were particle interactions, concentration of the phase volume, shear rate, particle shape and size, particle density and particle size distribution (PSD) (Genc 2003). When the composition of MRF has relatively low viscosity, it does not settle hard and can easily re – disperse (Choi 2012).

2.3 Magnetorheological Gradian Pinched Mode

The MGP working mechanism is similar with flow mode. However it has a different configuration of magnetic circuit design. Arranging the poles axially along the flow path and separating the poles by a non-magnetic spacer generates a highly non-uniform magnetic field.(F D Goncalves & Carlson, 2009). This type of pole arrangement, it will generate magnetic fibrils, which will chock the flow of MR fluid near the wall of the valve. The specialty of this mode is that the slope between pressure and velocity relationship in magnetic gradient pinch mode will increase as well as when magnetic field increase.

MGP valve allows MR fluids to flow through a circular orifice that supplied with high magnetic field gradient. Instead of hardening the fluid all through the valve, the non-uniform field just cements MR fluids close to the gap.(F D Goncalves & Carlson, 2009). The general attractive field quality will control the internal separation that such cementing happens, in this manner successfully ontrolling the hole width. This kind of control has known as the MGP pinch mode. Figure 2.5 (a) shows the arrangement of poles and the flow direction of MR fluid through the gap in magnetic gradient pinch mode valve. P is indicated as the pressure at the inlet and Q is flow rate through the valve. For (b) in Figure 2.5, the picture shows the high non-uniform magnetic field produces in MGP valve. The high non-uniform magnetic field produced is due to arranging the poles axially along the flow channel and separate the pole by a non-magnetic spacer.

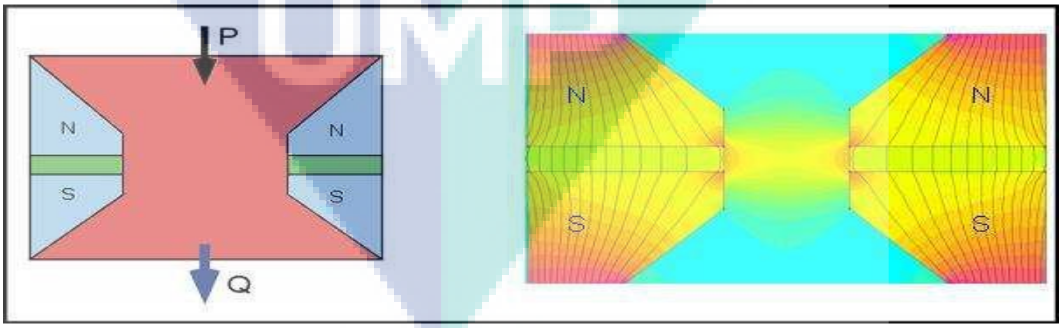

(a) (b)

Figure 2.5 (a) The Magnetic Gradient Pinch valve has poles arranged axially along the flow channel (b) High non-uniform magnetic field produced.

Source: (F D Goncalves & Carlson, 2009)

The MGP valve design by (Gołdasz & Sapiński, 2017) shown in Figure 2.6. The valve is axi-symmetic. (1) is the core, (2) is houses the coil, (3) is the flow channel and (4) is the non-magnetic spacer. The coil with current induces the magnetic flux in the core assembly that passes the core, will be directed to the flow channel. This type spacer-core-fluid arrangement will make the MR fluids choked near the flow gap walls.

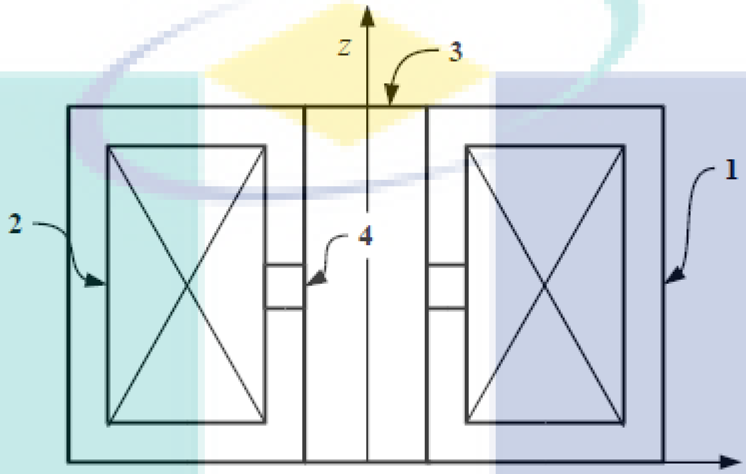

Figure 2.6 Pinch mode schematic layout 1=the core, 2= houses of coil, 3 flow channel, 4= non-magnetic spacer

Source: (Gołdasz & Sapiński, 2017)

According to (Gołdasz & Sapiński, 2017), the height of control valve is 20 mm, and the outer diameter is 21 mm. The diameter of outer flow gap is 4 mm. The non-magnetic spacer length is 2 mm. The size of coil window is 4x14 mm (width x height), and it incorporates N=150 turns of 0.51 mm dia. copper wire. The core material is low carbon steel alloy of the SAE 1010 grade, and the MR fluid's material characteristics are that of 26% Fe vol.

The configuration shows in Figure 2.6 incorporates three 2 mm long spacers to influence the distribution of magnetic field in the flow gap. And, the spacing sections length is 2 mm each. The coil and the core assemblies are identical with the design in Figure 2.6

The chock area of MR fluids will be near at the gap of MGP valve. The MGP valve that suitable for pinch mode are the valve with the circular orifice. The advantages of the circular orifice are, courser and larger magnetic particles can be used. The MR fluids valve should have a small diameter of gap but it cannot be too small. The circular orifice of the gap provides larger diameter then, larger and courser magnetic particles can be utilized in MR fluids. The rectangular orifice has too small diameter and when it use as a valve, the MR fluids will solidify through the entire gap when magnetic field is applied. This differs from circular orifice because the circular orifice will make the MR fluids solidify only at near of the gap, not through the gap like the rectangular orifice.

The benefit of the feature of the circular MGP valve compared to a normal MR fluid valve which is rectangular orifice is the potential to have a much lower viscous off-state. The viscous flow loss of a single 2 mm MGP orifice is considered smaller than the flow loss experienced with the narrow gap (~0.5 mm) found in many MR fluid valves. This may be paradigm shifting with regard to desirable or necessary fluid properties. (F D Goncalves & Carlson, 2009).

CHAPTER 3

METHODOLOGY

3.1 Introduction

This study involves simulations, design of experiments, optimizations, fabrication and evaluation. The methodology of research were conducted in three stages namely the concept development; magnetic field simulation and design optimization; and fabrication and evaluation.

3.2 Research flow

As depicted in Figure 3.1, the research started with comprehensive review of previous MR valve design. Evaluation of the previous design was conducted as a point of departure for the development of a new concept design. Concept designs was prepared in three options with consideration of pinched mode as a basic design principle. The concept designs then analysed for magnetic strength and distributions using finite element analysis. An open source software named as Finite Element Method for Magnetic was used to obtain the magnetic model. A final concept design was developed based on design evolution as presented in every proposed concept.

Next second of the project was an optimization of geometrical parameter using response surface methodology approach. The third stage was the optimized prototype fabrication and evaluation. Evaluation involve fabrication tolerances and generated magnetic field strength. Materials used to fabricate the prototype are mild steel, aluminium, magnetic wire, fastener, oil seals, hydraulic fitting/hose, and pressure meters. Measurement of the generated magnetic field strength was conducted using a handheld magnetometer. The measurement is significant to calibrate the magnetic circuit control system. In order to produce the magnetic field, an AC-DC power supply with ability to constant the current of 0.1 to 5 A was used.

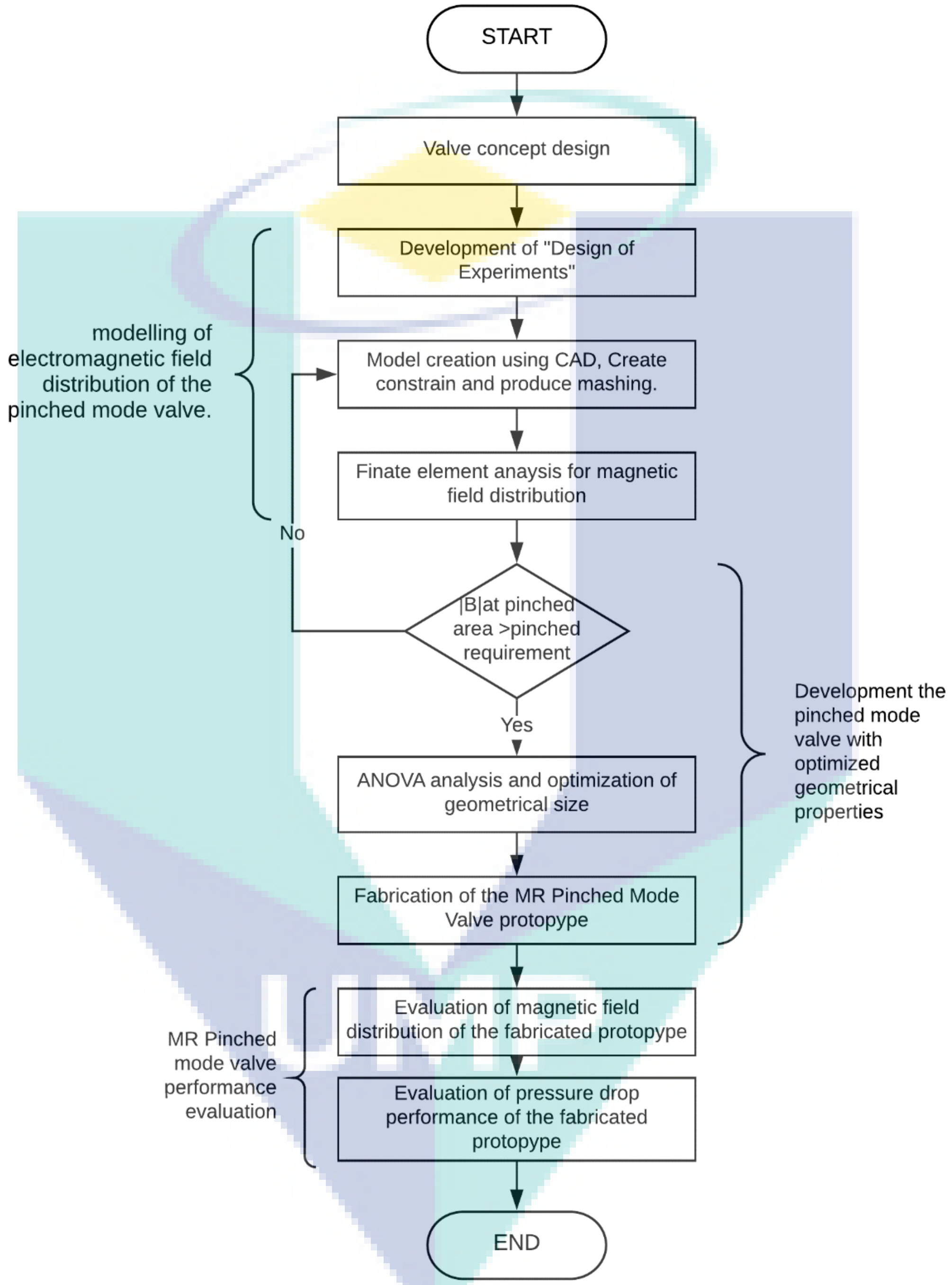

Figure 3.1 Process flow of the project.

Final stage of the research will be a pressure drop performance evaluation of the prototype. The evaluation will be conducted using commercial MR fluid (MRF- 132DG) and inhouse made MR fluid (Mineral-Oil based MR fluid). The results from MRF-132DG will be a benchmark of commercial materials. To prove the performance of the pinched mode valve at wide range of MR materials compositions, an experimental based measurement will be conducted using the Mineral-Oil based MR fluid. The Mineral-Oil based MR fluid composition of Carbonyl Iron Particle (CIP), Mineral Oil and Surfactant will be synthesized using Mixture Design of Experiments. Each components of the MR fluid will be analysed for particle size distribution using particle sizer machine and scanning electron machine. Prior experiments, all MR materials will be analysed for rheological and magnetic properties using Antoon Paar Magnetic Rheometer. To conduct the experiments, a magnetorheological dynamic testing machine will be used. Response of pressure drop from the experiments will be analysed to plot the performance of novel pinched mode device.

3.3 Design Concept

Design process started with concept development of pinched mode magnetic circuit. Direction of the concept development is focus on achieving strong magnetic field at the pinch region while maintaining large gap between pole. The concept design requirement that have been prioritize were:

- 5-6 mm annular diameter of MR fluid (to comply standard parts dimension)
- Average values of magnetic flux must be more then 0.06 Tesla
- Modular device fittings

The concept design than selected based of design requirement and feasibility to be fabricated. The selected design geometry than drawn in CAD software for FEA analysis. A full factorial design of experiment were developed for geometry optimization. Figure xx shows the selected concept design that developed in this study.

The value of magnetic flux readings is also taken into account where the value of MRF is directly proportional to MRF commercial value. In this study, the MRF used was modified according to the mixtures of MRF additives (Zhao-Dong Xu 2014). The final component of MR pinched mode valve was divided into three parts namely non-magnetic, magnetic and electromagnetic coil. Non – magnetic was used in parts 3 and 4 see figure 3.2. The use of these non – magnetic materials were act as a protector to the MR fluid from making contacts to the coil. It also guides the magnetic flux to the effective area. Furthermore, magnetic materials were used in part 1 in order to guide and give the effect of magnetic dispersion. It also increase the magnetic field depending on current supply and winding coils. The summary of the materials are shown in Table 3.1.

C-magnet is the part will give the magnetic reaction which is the main objective in this study. The design development was continued by identifying geometry for C-magnet. This section is described in detail in subchapter 3.3.3. The geometry of proposed design are chosen based on stability of product to manufacture and the effect of magnetic field at the presence and absence of MR fluid.

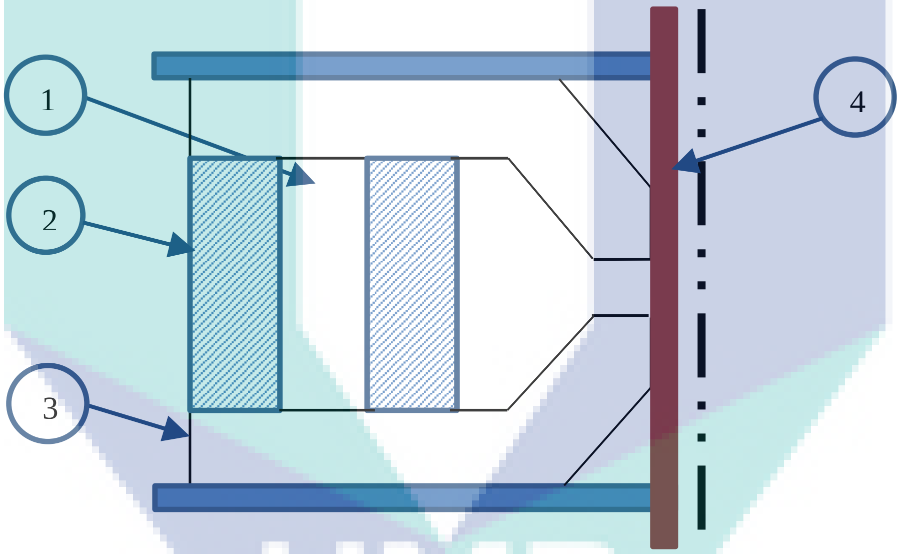

Figure 3.2 Selected concept design of pinched mode valve

Table 3.1 List of parts and materials of MR Pinched Mode Valve

Part No.	Part Name	Type of Material	Material	Type
1	Core	Magnetic	Low Carbon Steel	S20C
2	Coil	Non-magnetic	Copper wire	22 AWG
3	C-Magnet	Non-magnetic	Stainless Steel	None
4	Tube	Non-Magnetic	Copper	None

In detail, the current outer length of magnet is 60 mm and its outer width is 57 mm. The core gap is 5 mm, core length is 34.3 mm and the coil width is 7.5 mm. The magnet material is mild steel and the channel material is stainless steel. The copper wire have been selected in supplying a current which 3A in control. It also incorporates 320 turns of 0.644 mm diameter, 22 AWG to influence the magnetic field distribution in flow gap. The effective area of a channel is 8 mm.

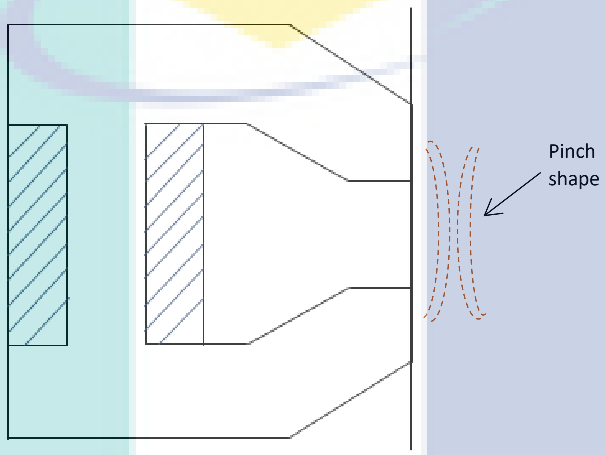

Figure 3.3 Concept design of the pinched mode device

3.4 Finite Element Model Design

The finite element model design is about the design and simulation of the MGP valve under a magnetic field that been induced by the coils inside it. The magnetic flux and magnetic strength intensity can be calculated at each element node. So, the area of high density of magnetic strength will be analysed to observe the diameter of effective.

The first step is to make a finite element model design in FEMM. MGP valve is categories in low frequency magnetic problem. This software helps to construct the design shape, materials properties, circuit properties, boundary properties, mesh analysis generator, type of problems and finally finite element analysis. Definition of a problem was set as shown in Figure 3.4. Problem type of planar with the length unit in millimetre. As the valve runs in DC power supply.

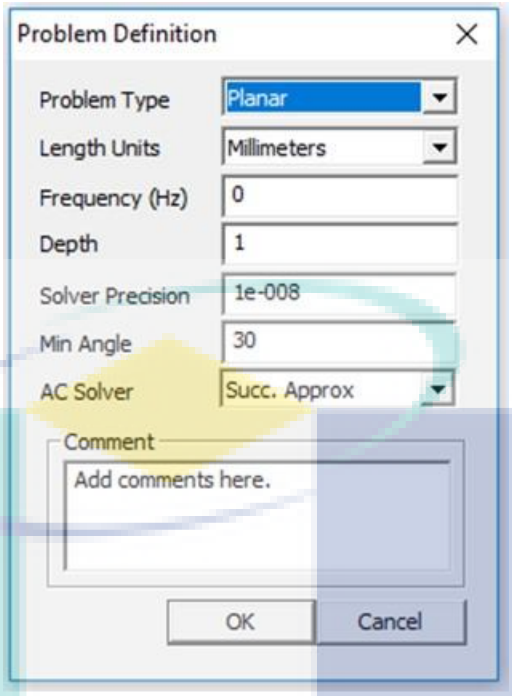

Figure 3.4 Problem Definition for Finite Element Model Design

Then, the second step is materials selection as in Figure 3.5. The materials are pure iron as the conductor that categorize as soft magnetic materials. Soft magnetic is a materials that easily magnetize and easily demagnetize. It is very suitable for MGP valve because during off-state condition, there is no need for any magnetic field because it can disturb the performance of the valve. The coil winding is using 22 AWG copper wire and MRF-132 DG as the fluid that flow through the MGP valve and air as medium to fill the blank space.

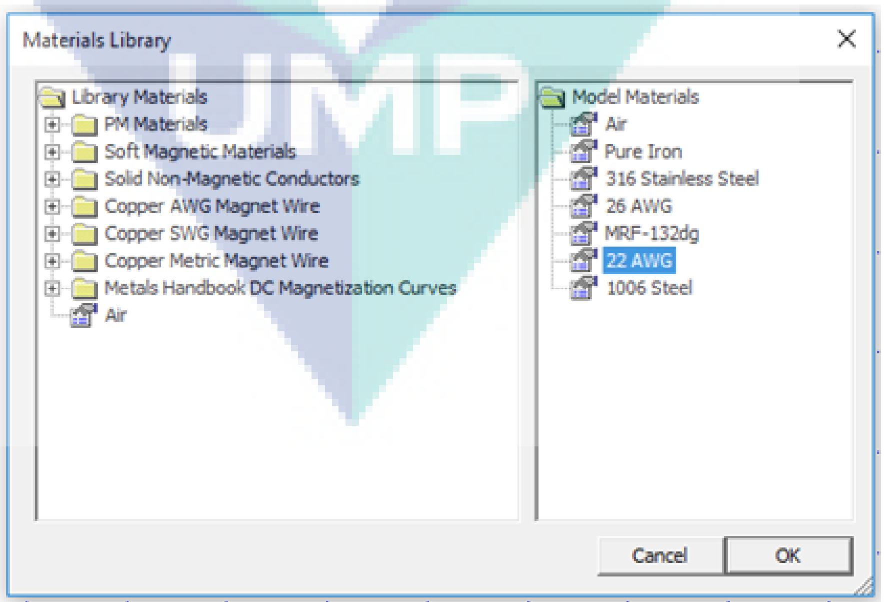

Figure 3.5 Material Library for Finite Element Model

The valve geometry is characterized as shown in Figure 3.6 by the W_o is outer width, W_c is for coil width, C_p is core gap, L_c is core length and L_o is outer length. D_{eff} is for effective diameter in the choke area of channel. The finite element model will be analyzed as a 2-D planar model. In this software, there are material library which help to select any materials for the core, valve housing, flow channel and the coils.

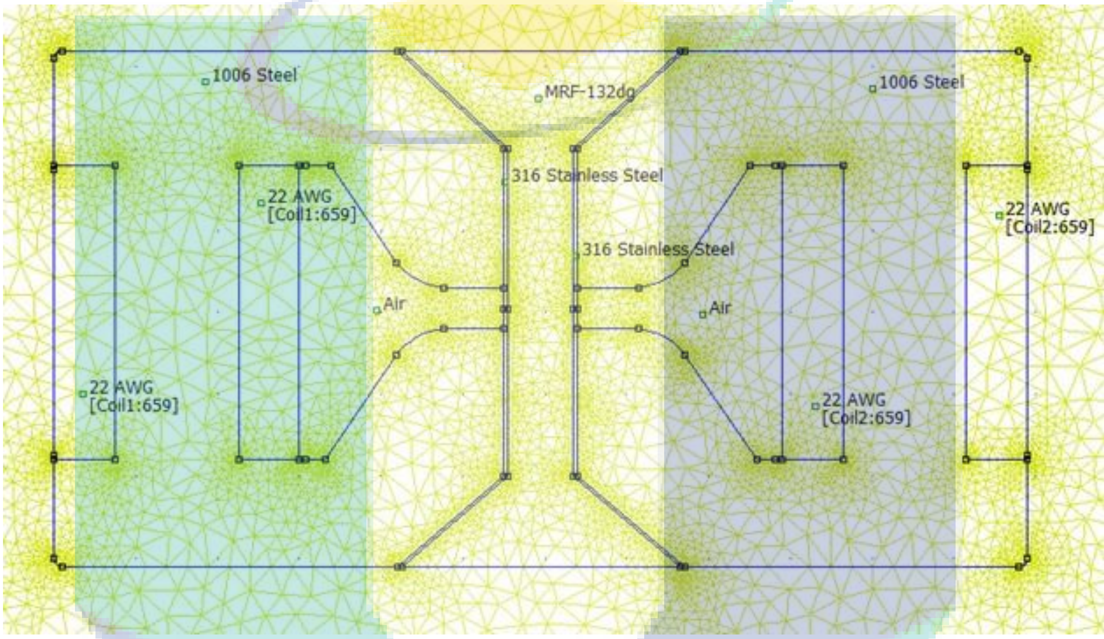

Figure 3.6 Geometry Characteristics of Finite Element Design for MR pinched mode valve

Furthermore, turning wire is also an important parts that affects the magnetic field distribution. Thus, to determine the exact number of turning wires, a few mathematical modeling were required. This modeling was done after ensuring the height and width of C-magnet which is suitable based on the previous study. Figure 3.7 shows schematic diagram in determining the number of turn coils and wire diameter based on core geometry.

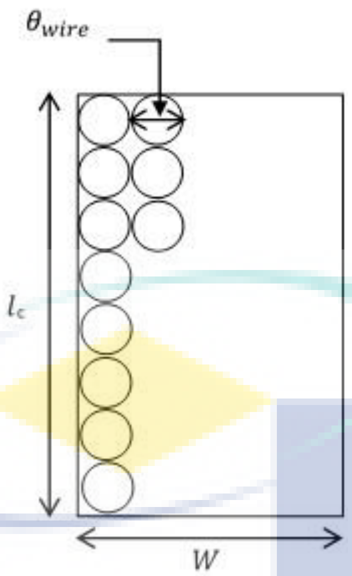

Figure 3.7 Schematic diagram of mathematical modelling

Then, this study come out with the mathematical formula in order to get the right turning coil. Equation 3.1, 3.2 and 3.3 shows the method to get the turning coil value.

$$n = \frac{l}{\theta_{wire}} \tag{3.1}$$

$$l_T = \frac{W}{\theta_{wire}} \tag{3.2}$$

$$N = n \; x \; l_T \tag{3.3}$$

The properties of the circuit for the coils is determined in the circuit properties for the current applied, the direction of the current and type of connection whether series or parallel. From this features, modification of the magnetic circuit can be done.

3.4.1 Simulation of Magnetic Circuit

In this study, Finite Element Magnetic Method (FEMM) was used to simulate and analysed the magnetic field for electromagnetic circuit design for pinched mode valve. FEMM is a finite element package for solving two-dimensional planar and axisymmetric problems in low frequency magnetics and electrostatics. The main purpose of using finite elements is to break the problem down into a large number regions, each with a simple geometry (Meeker 2010).

If enough small regions are used, the approximate potential closely matches the exact solution. The advantage of breaking the domain down into a number of small elements is that the problem becomes transformed from a small but difficult to solve problem into a big but relatively easy to solve problem. Through the process of discretization, a linear algebra problem is formed with perhaps tens of thousands of unknowns. However, algorithms exist that allow the resulting linear algebra problem to be solved, usually in a short amount of time.

In detail, FEMM discretizes the problem domain using triangular elements. Over each element, the solution is approximated by a linear interpolation of the values of potential at the three vertices of the triangle. The linear algebra problem is formed by minimizing a measure of the error between the exact differential equation and the approximate differential equation as written in terms of the linear trail functions.

After placing all the material properties and setting the boundary conditions, the two-dimensional of MR pinched mode valve model was finally meshed with a coarse triangular mesh at the outside region and a finer triangular mesh at the specific regions such as pinch area as shown in figure 3.8.

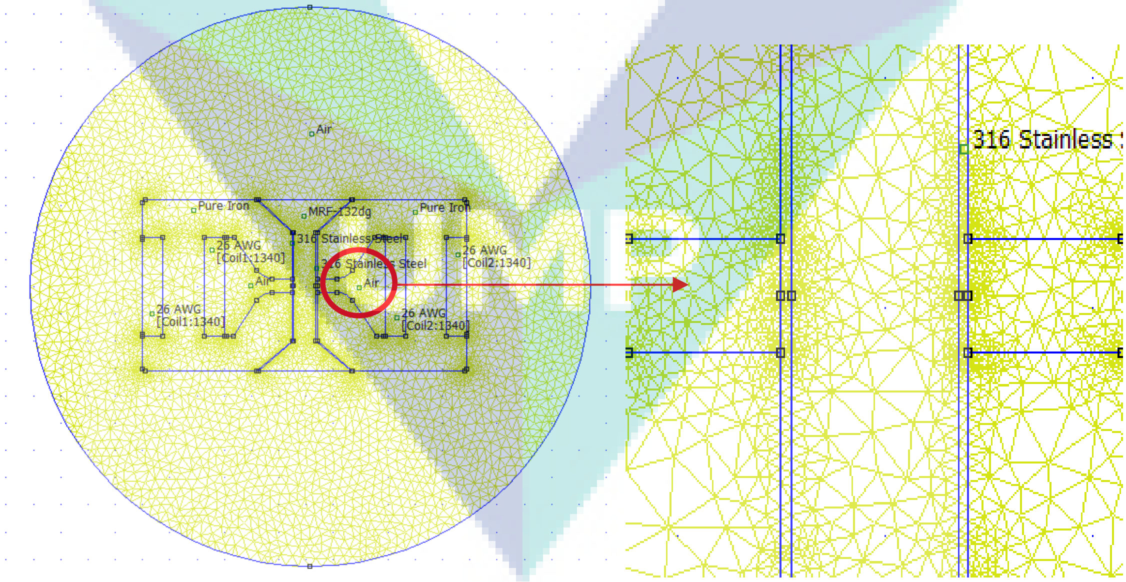

Figure 3.8 Meshed geometry in FEMM

The properties of non-magnetic materials, such as stainless steel, copper wire and air were assumed to be linear. Meanwhile, the magnetic properties for magnetic materials such as stainless steel and MRF 132 DG were assumed to follow the B-H curve given by the software package and provided by the manufacturer. This software package was related to the type of material for each component of the MR pinched mode valve, number of turning coils and the values of the control coil current supplies. All these parameters were important to produce the best value of the magnetic flux density, B(Gołdasz and Sapiński 2017). Then, the simulated magnetic flux distribution are then presented in the form of flux density contour maps that shown in the figure 3.8.

3.4.2 . Measurement of magnetic properties

The use of FEMM software in this study is to discretise the geometry. Examining MR pinched mode valve is characterized by the axial symmetry so that the field problem can be solved in the two-dimensional formulation. The magnetic field analysis at the pinch area was a magneto static problem in which the field are time-invariant. In this case, the field intensity, H and flux density, B must obey equations 3.4 and 3.5, respectively as below:

$$\nabla \times H = J \tag{3.4}$$

$$\nabla \cdot B = 0 \tag{3.5}$$

Equation 3.4 and 3.5 subject to a consecutive relationship between B and H for each material as shown in equation 3.6 below:

$$B = \mu \cdot H \tag{3.6}$$

FEMM goes about finding a field that satisfies an Equations 3.4 to 3.6 via a magnetic vector potential approach. Flux density is written in terms of vector potential, A, as in Equation 3.7:

$$\beta = \nabla \times A \tag{3.7}$$

Adopting the B and H relationship in Equation 3.4 and flux density in Equation 3.6, Equation 3.5 can be written as Equation 3.8:

$$\nabla \times \left(\frac{1}{\mu(B)} \nabla \times A\right) = J \tag{3.8}$$

FEMM retains the form of Equation 3.8 for the purpose of solving magneto static problems with a nonlinear B and H relationship. The sample to be used in FEMM 4.2 software was MRF-132DG and the B and H relationship of the sample is shown in Figure 3.9. The nonlinear curve was then plotted and was defined under property of materials in the software. Hence, Equation 3.8 was used for this analysis due to the nonlinearity.

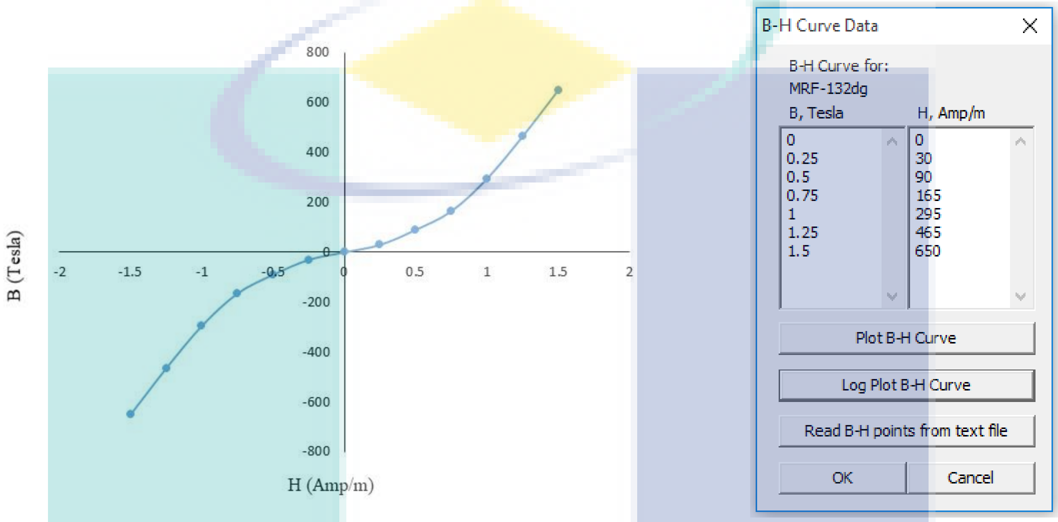

Figure 3.9 *B-H* curve of MRF-132DG (Rubber 2015) and its data defined via FEMM

3.5 2 – Level factorial design (DOE)

The DEO began by identifying variable geometry parameters and the responses of the instrument. The parameters included were core length, outer width, coil width and pinch gap which calculate in millimetre unit. These design geometries were chosen after considering their suitableness of ease of manufacturing and assembly. However, a systematic design optimization method is needed to successfully fabricate the best device. Here, the Design Expert 7.0.0 has been used to optimize the geometry parameters.

There are many types of factorial experiment. In this study it will restrict to the 2-Level Factorial Design; 2^n factorial experiment to optimize the design geometries where n is the number of experimental variables. The method of factorial experiment is being utilize for estimating main effects and interactions which gives the levels of the experimental variables from the lower level to the upper level. In the other hand, this 2-Level Factorial Design provides an effective means for screening through many factors to find the critical few. These designs permit estimation of all main effects and all interaction effects.

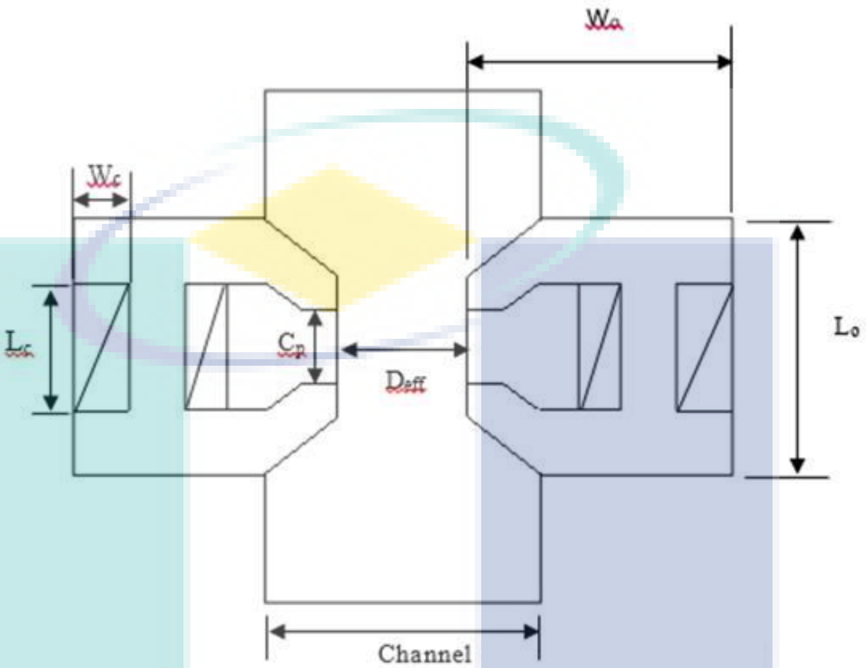

Figure 3.10 Illustration of the 2D final generation of the new MR pinched mode valve.

In this study, 2^4 factorial has been decided as well as the four variables has been decided as the variable geometry. They were then categorized to two different lower and high level as shown in Table 3.2.

Table 3.2 Low and high of geometry parameters

No.	Name	Units	Type	Low	High
A	Outer Width	mm	Numeric	54	57
B	Coil Width	mm	Numeric	6.5	7.5
C	Core Length	mm	Numeric	33	37
D	Pinch Gap	mm	Numeric	5	9

Then, three responses were considered as minimum magnetic flux, maximum magnetic flux and ratio (min and max). All responses were analysed who rated the magnetic flux on a scale 0 to 10. This is a linear transformation to make data entry and analysis easier. All the responses were read in Tesla unit. From the 2^4 factor, it were comprise with 16 experiments. The results from running all combinations of the chosen geometry parameters as shown in Table 3.3.

Table 3.3 Geometry of each parameter

Sample No.	**A: Outer Width (mm)**	**B: Coil Width (mm)**	**C: Core Length (mm)**	**D: Pinch Gap (mm)**
1	57.00	6.50	37.00	5.00
2	54.00	7.50	37.00	9.00
3	54.00	6.50	33.0	5.00
4	57.00	7.50	33.00	9.00
5	57.00	6.50	37.00	9.00
6	54.00	6.50	33.00	9.00
7	57.00	7.50	37.00	5.00
8	54.00	7.50	37.00	5.00
9	54.00	7.50	33.00	9.00
10	54.00	6.50	37.00	9.00
11	57.00	7.50	33.00	5.00
12	57.00	6.50	33.00	9.00
13	54.00	6.50	37.00	5.00
14	54.00	7.50	33.00	5.00
15	57.00	6.50	33.00	5.00
16	57.00	7.50	37.00	9.00

The data for all factors geometry based on the design drawing that has been finalized. Furthermore, the second column in Table 4 show the sixteen experiments that need to be simulated by using Finite Element Magnetic Method (FEMM) software. These sixteen experiments were to fulfil the data for three responses that already considered. Moreover, the ratio of magnetic flux have been determined based on the mathematically calculation below:

$$Ratio\ of\ magnetic\ flux = \frac{Response\ 1 + Response\ 2}{2}$$

3.6 Simulation

Based on parameter generated for the DOE, a parametric cad drawing were developed. The CAD drawing then imported to Finite Elements Method Magnetics (FEMM) software. Then, the boundaries condition, materials and circuit definition were specified. Triangular mashing than generated and finally magnetic field simulation were conducted. The simulation were conducted based on 2D-planar model. Process of magnetic field simulation is shown in Figure 3.11.

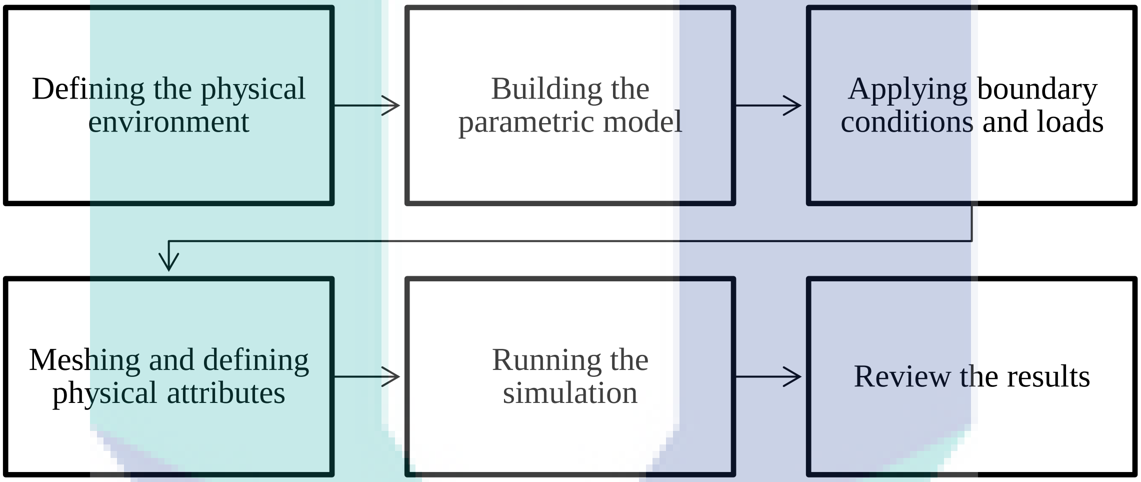

Figure 3.11 Finite element modelling process steps.

All parameters were selected to produce the best value of magnetic flux density, B, across MR fluid in MGP valve. In addition, the magnetic properties of the magnetic material are assumed to follow the B-H curve given in the FEMM software.

At the modelling and design stage, all parameters including selection of materials, fluid gap, diameter of fluid channel, number of turn winding coil as well as the flux length need to be considered. All these parameters correlate to the main purpose of the electromagnetic coil design in MGP valve whom to achieve optimum magnetic flux density at the effective areas, that is pinch or choke area.

In selecting the best design of pinched mode mechanism, some of parameter have been set as the fix parameter and the rest being set as the parameter changes. This is due to ensure the best effectiveness magnetic field distribution at the choking area.

The material of each component were choose based on their criteria. In practical, a gap less than 0.5 mm has been said as very easy gap to manufacture and assembly (Fernando D. Goncalves, Ahmadian, & Carlson, 2006). In this study, the gap have been set from the range of 5 mm to 9 mm with fix of current apply at 5A which is based on the magnetic field distribution.

Further analysis of the simulated results were conducted to measure magnetic field strength along the gap. The results were treated as response of geometrical changes in the design. In magnetic circuit with an air gap, the strength of the magnetic field B, depends strongly on the length of the air gap.

3.7 Fabrication

Fabrication process involved four difference stages namely, core machining; core winding, housing machining, assembly. Figure 3.xx shows components of the testing rig that involved in the fabrication process. The core was made from mild steel using CNC milling and EDM wire cut method. Eight pieces of the core caps were made separately and then press fit joined together with core bar to produce four set of solenoid.

Winding process involve magnetic wire with gauge number of AWG 22. The magnetic wire was winded tightly to produce xx number of turns. The housing of the rig was made through rapid prototyping process. Purpose of the housing is to secure the position of the solenoid and other components.

3.8 Evaluation of the pinched mode MR valve

Evaluation of the fabricated testing rig was conducted using magnetometer at various current supply. The evaluation process stared preparing apparatus as depicted in figure xx. Magnetometer was placed perpendicularly with magnetic field at the effective gap.

Due to small ration between probe size to effective gap size, the measurement were taken at 5 location only. Location of measurement is shown in figure xx. Next, constant DC electric current of 0.2 A were supplied on the magnetic circuit to produce magnetic field. The value of electric current were maintain for all 5 location of measurement. The process repeated for other value of electric current from 0.2 A to 2 A with 0.2 A interval. The collected data then plotted and compared with simulation result.

3.4 Experimental works

Figure 3.12 shows the diagram of MR pinched mode valve instrument. The instrument mainly consist of DC power supply, new fabricated MR pinched mode valve, Gaussmeter and tank. A single output DC power supply is connected directly to the fabricated device. It has an operating voltage up to 10 V and 1.4 A. The gauss meter used is transverse type. This is due to the consideration on the magnetic flux dispersed.

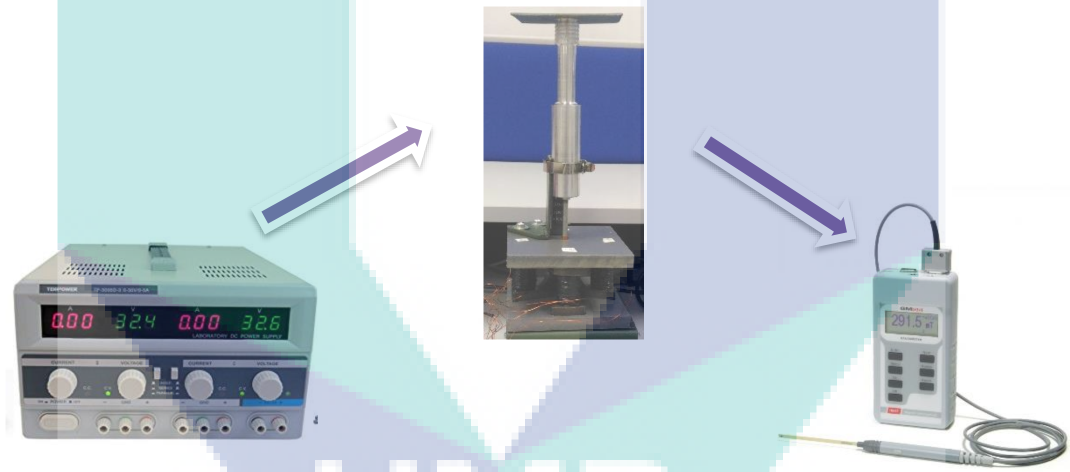

Figure 3.12 The instrument and the connection of the experimental work

Figure 3.13 shows the way of gauss meter usage. The gauss meter are attached to the copper tube where the effective area was suspended (green circle). The reading of magnetic flux were taken with the several of current supply.

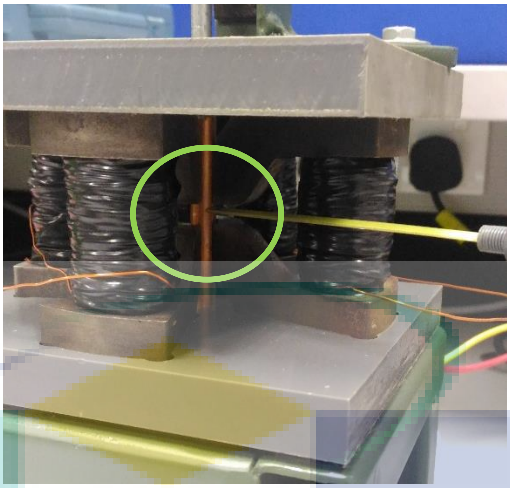

Figure 3.13 The effective area (green circle)

Figure 3.14 Full set up of the experimental apparatus

Figure 3.14 shows the full figure of apparatus set up continuity from the figure 3.18. Power supply be the main factor in order to get the best value of magnetic flux. The resistance effect from coil wire is checked before the experiment is run. The calculation of resistance as per equation 3.9.

$$\text{Total resistance} = \frac{1}{R_1} + \frac{1}{R_2} + \frac{1}{R_3} + \frac{1}{R_4} \tag{3.9}$$

where the resistance refer to the coil winding for the first core and continue with the next core part.

The test were performed by applying the current to new MR pinched mode valve with the absence and presence of magnetorheological fluid sample who being accommodate in the cylinder part. The test were started when load have been applied on the load stand. This is intended to put pressure on the cylinder to push down magnetorheological fluid. The magnetic flux value is taken using the gaussmeter and the pressure value is taken as well as the load on the cylinder. All the value of magnetic flux and pressure is taken at current value 1.4 A in control

CHAPTER 4

RESULTS AND DISCUSSION

4.1 Introduction

This chapter includes all the results and discussion throughout all the research. Concept design development and modelling in both 2D and 3D environment were conducted and evaluated. Discussion on geometry optimisation comprising response measurement through finite element analysis is presented here. Optimisation of geometrical parameters conducted to obtain the best parameter value for the device before went through the fabrication process. The following section presents the fabrication outcome of the prototype which are the physical properties and magnetic field measurement. Section 4.4 explains the performance evaluation of the pinched valve. The effects of magnetic field strength on the pressure drop are discussed.

4.2 Concept design development and modelling

There are three concepts explored to develop the idea of pinched mode valve. Magnetic field distribution of each concept was simulated where each concepts design is independent and able to produce a chocked mechanism for MR fluid pinching purpose. The concepts were not designed to be selected but rather to provides knowledge of good design in the final concept.

The concept design started with the initial idea to achieve a concentrated magnetic field around choking area. All concepts are resulted in the following descriptions:

Concept 1

Concept 1 was developed based on 'u' shaped magnet as shown in figure 4.1. Simulation result of magnetic field distribution as depicted in figure 4.2 shown the magnetic field is diverted to the tip of the magnetic disk.

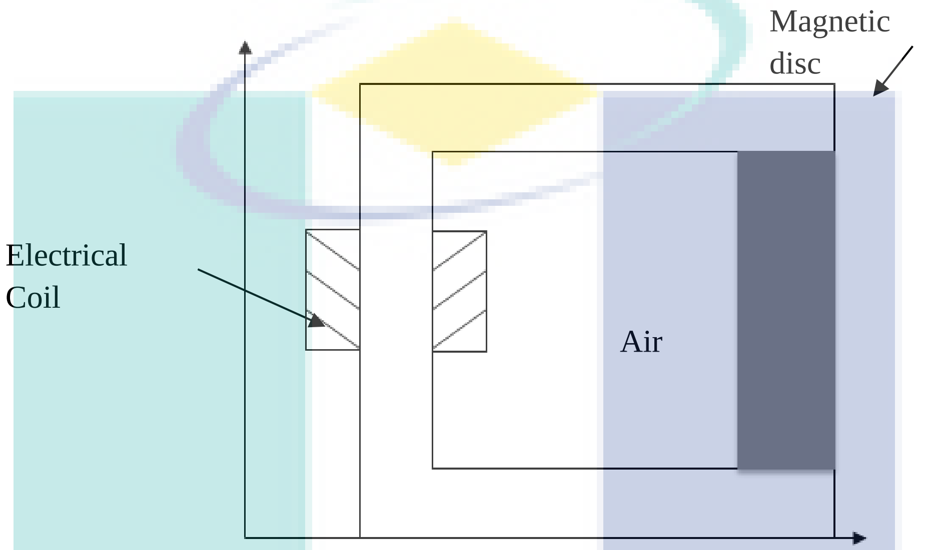

Figure 4.1 Schematic drawing of two dimensional axisymmetric-model of concept 1

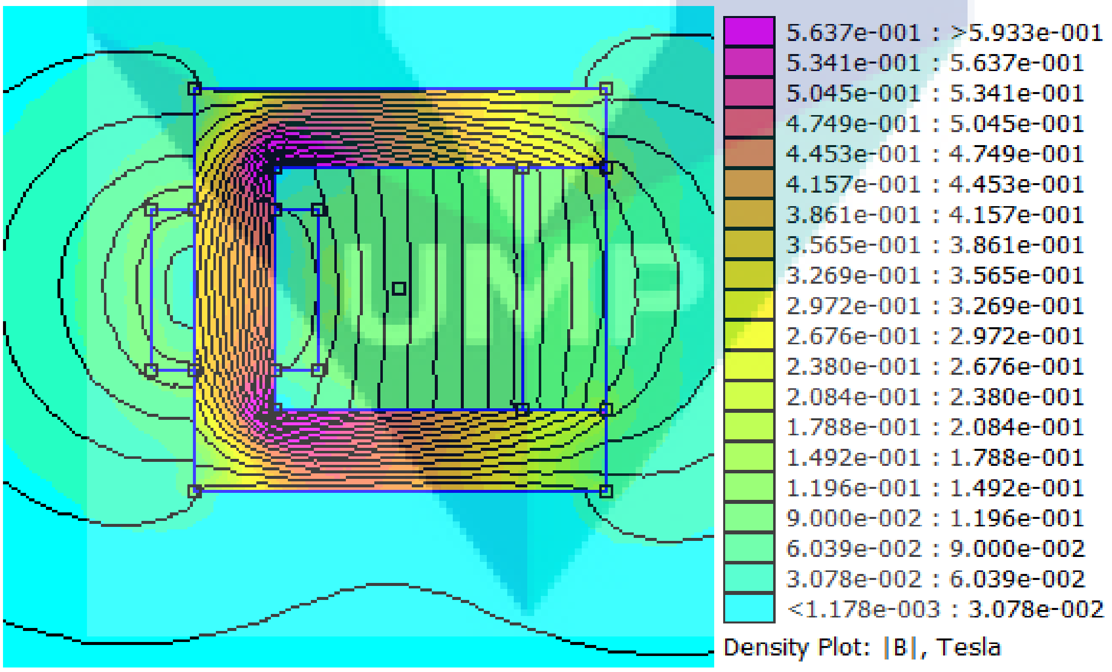

Figure 4.2 Magnetic flux density contour of concept 1

Concept 2

Concept 2 was developed by enlarging the size of the magnetic disk, as shown in figure 4.3. The result of magnetic field analysis as shown in figure 4.4 indicate

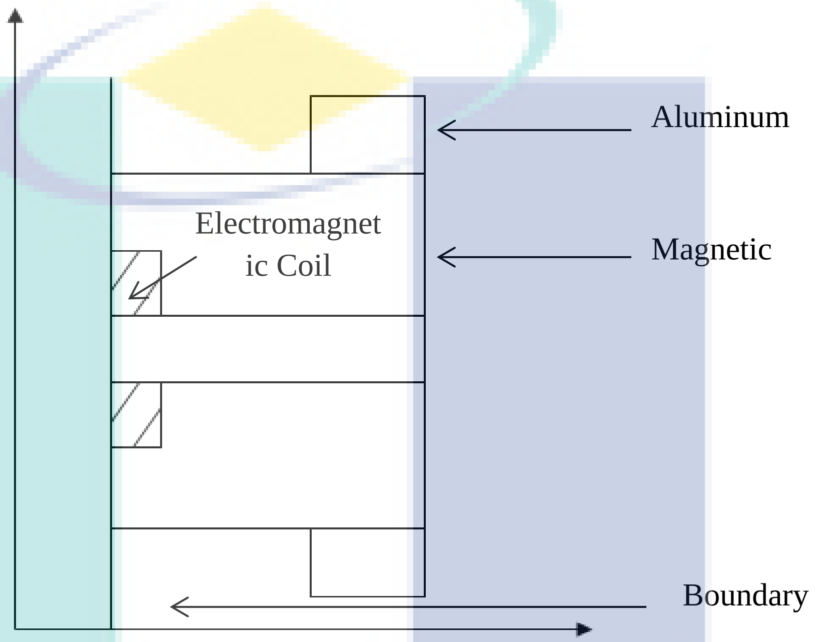

Figure 4.3 Schematic drawing of two dimensional axisymmetric model of concept 2

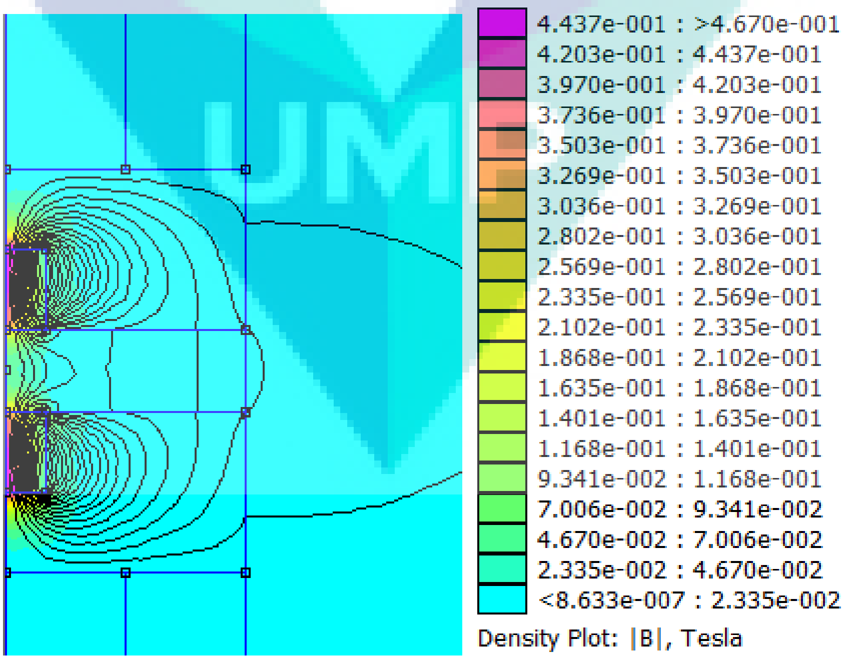

Figure 4.4 Magnetic flux density contour of concept 2

Concept 3

The third concept was produced based on the idea of enhancing the first and second concept by reducing the magnetic gap between pole end as depicted in figure 4.5

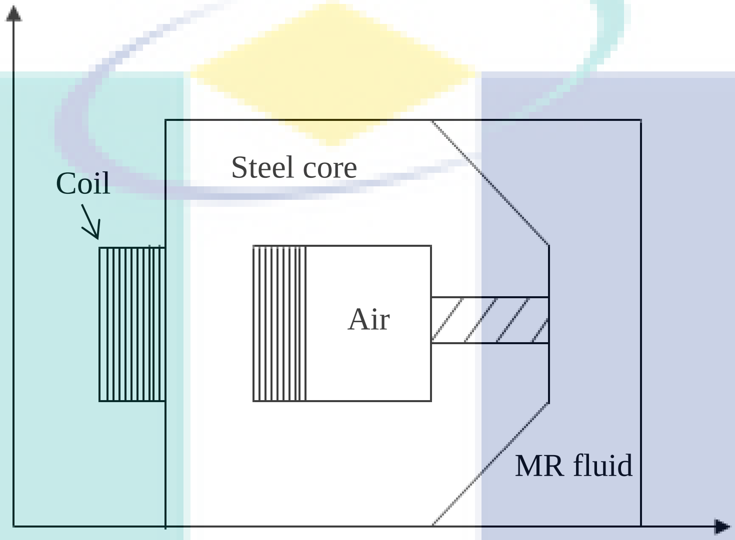

Figure 4.5 Schematic drawing of two-dimensional axisymmetric model of concept 3

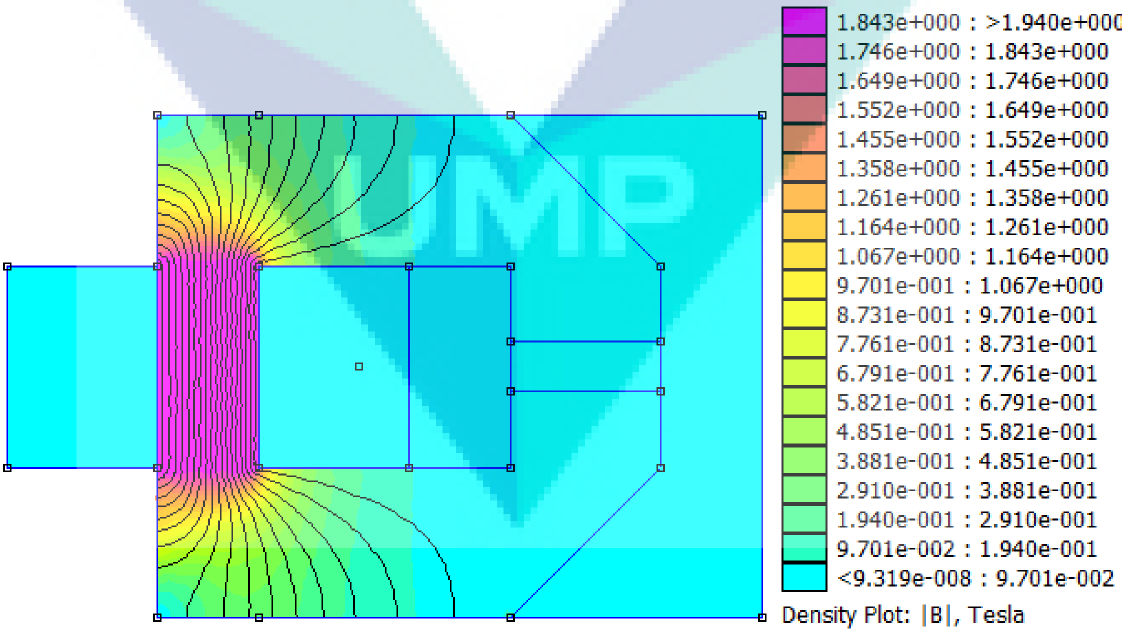

Figure 4.6 Magnetic flux density contour of concept 3

4.2.1 Modelling of electromagnetic field distribution of the pinched mode valve

Meshing and boundary condition definition of electromagnetic field distribution of the pinched mode valve that based on the third concept is shown in figure 4.7. The meshing process produced 15894 nodes

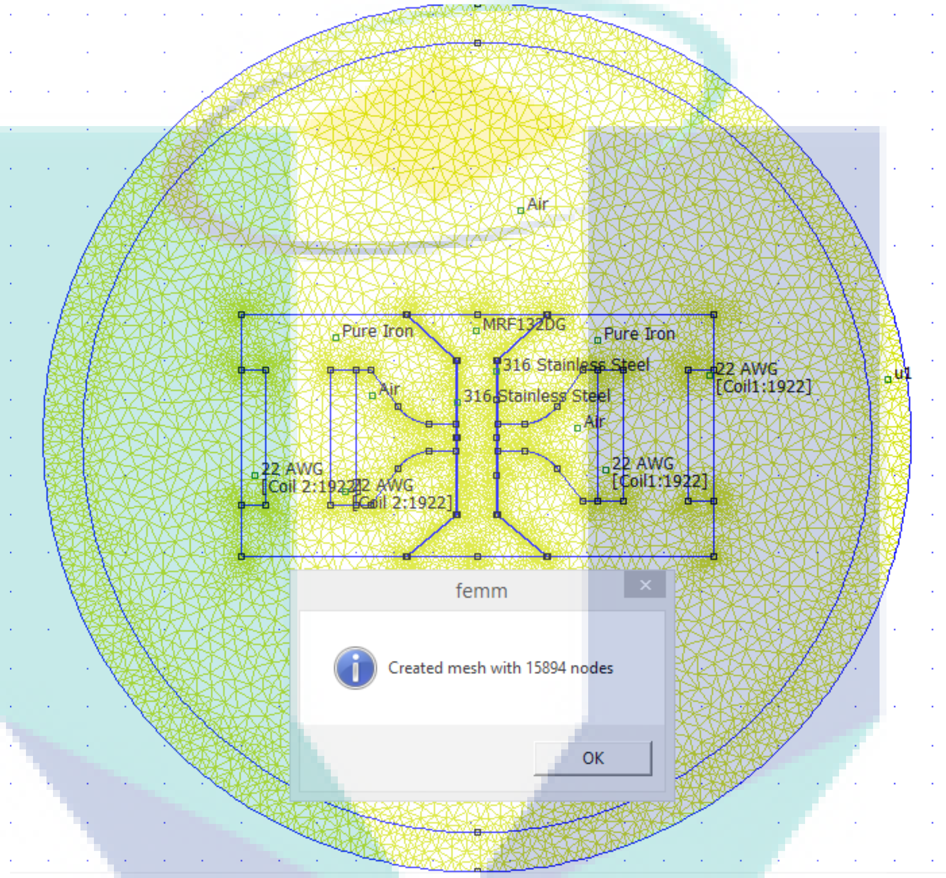

Figure 4.7 Meshing and boundary condition of the simulated model.

There are 16 runs for the simulation of MGP valve using FEMM software. Results of all simulation are shown in figures 4.2 to figure 4.32. The figure indicates the magnetic flux density that covers the area of MGP valve and magnetic field plot at the centre of choking gap (red line). The highest and the lowest of magnetic flux are at 0.97 Tesla and 0.39 Tesla respectively. Similar trend found in all 16 runs but at different values. The results shown in table 4.1

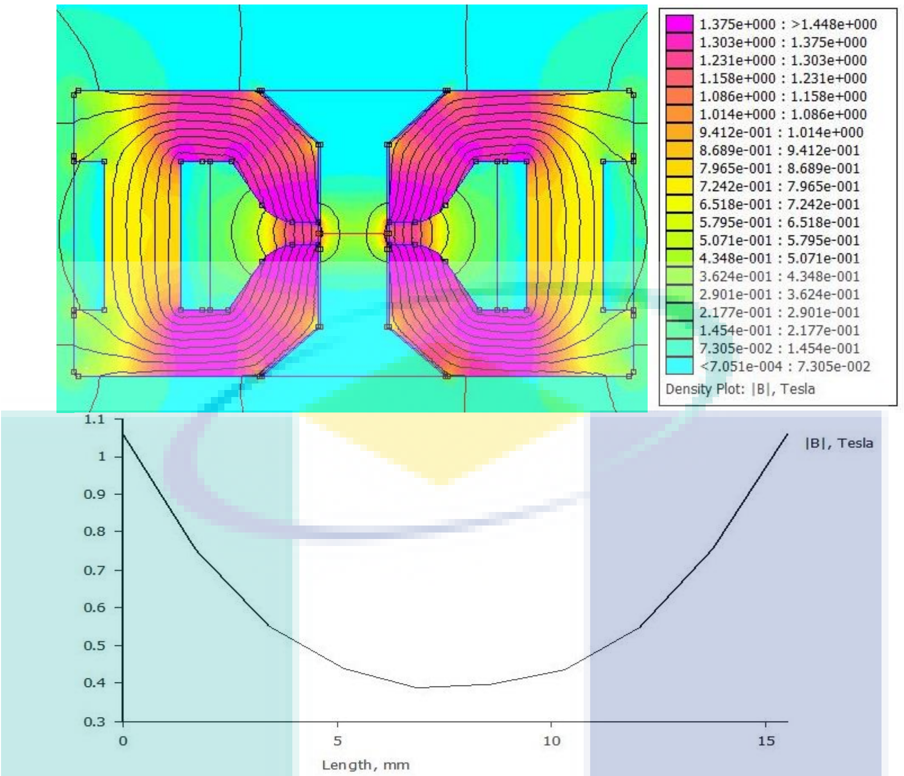

Figure 4.8 Magnetic flux distribution for sample 1

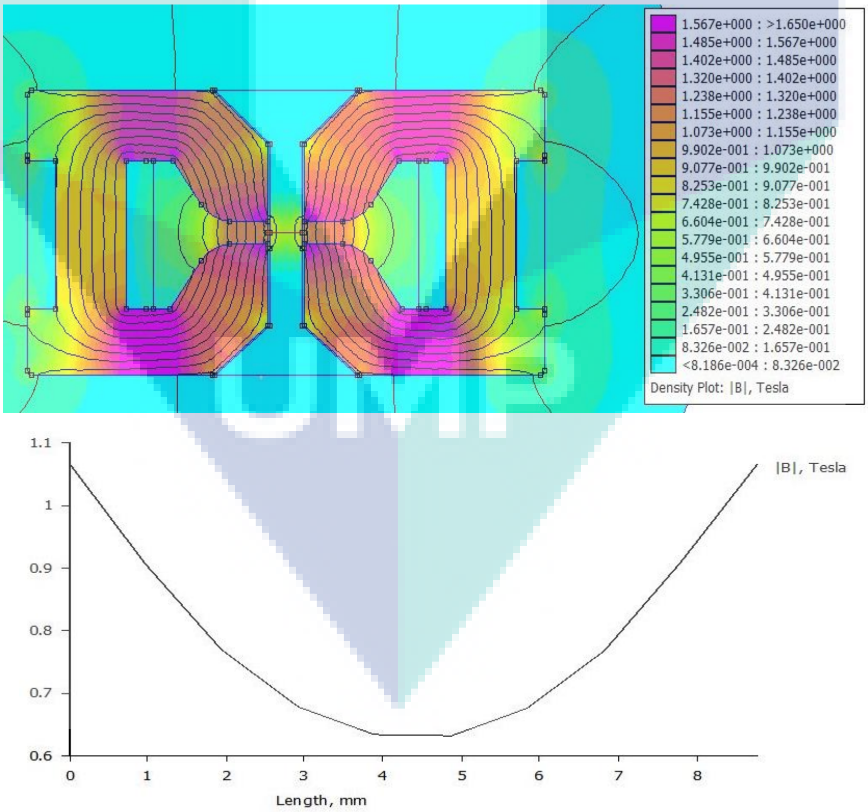

Figure 4.9 Magnetic flux distribution for sample 2

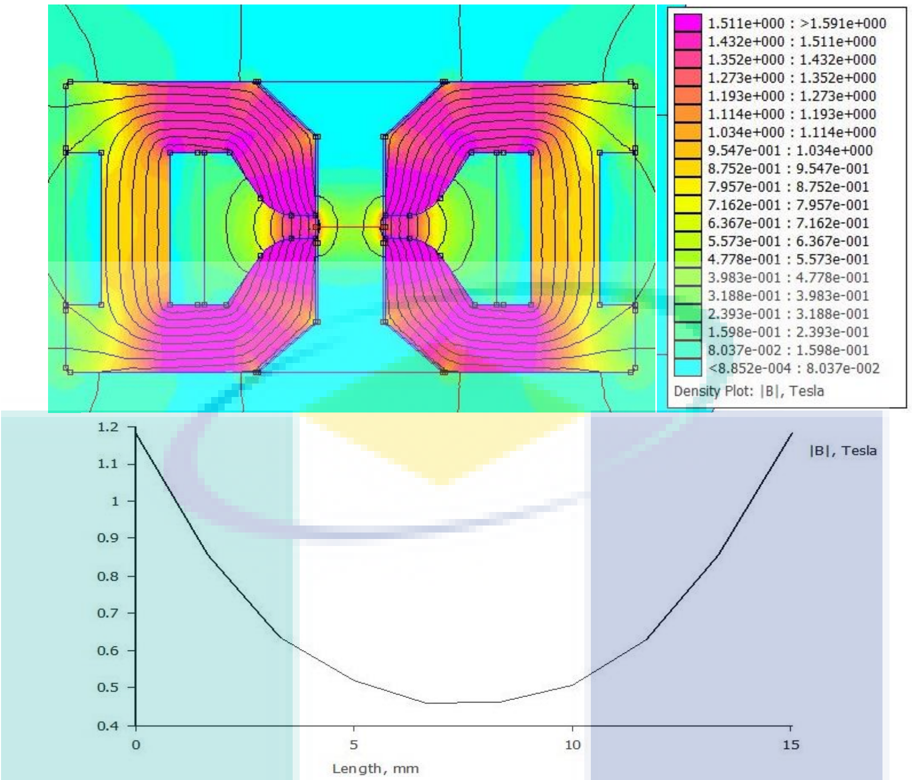

Figure 4.10 Magnetic flux distribution for sample 3

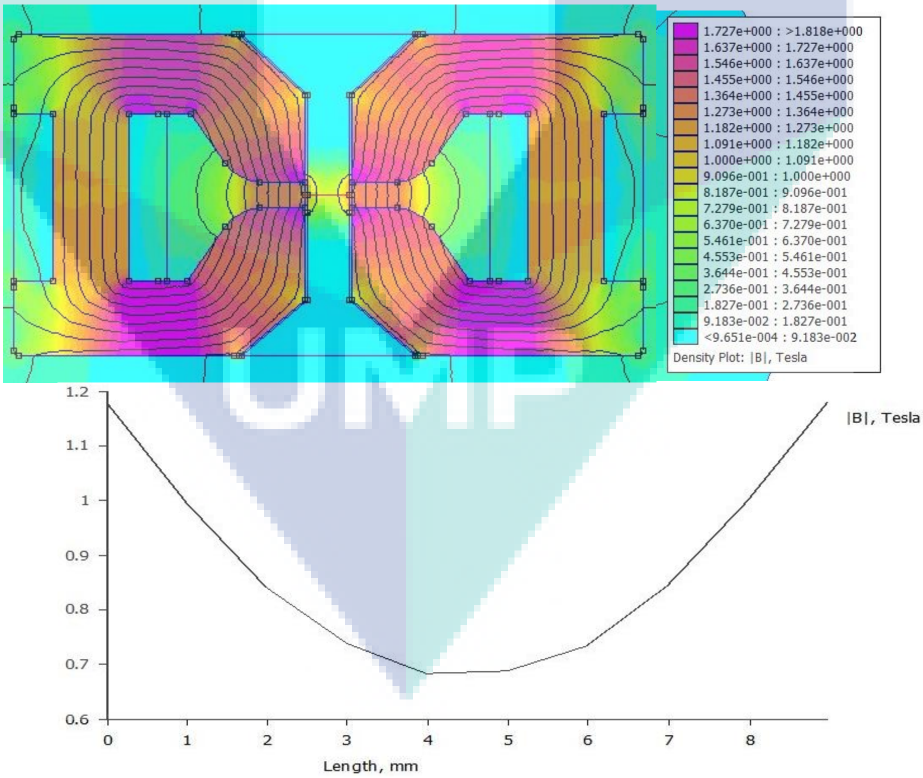

Figure 4.11 Magnetic flux distribution for sample 4

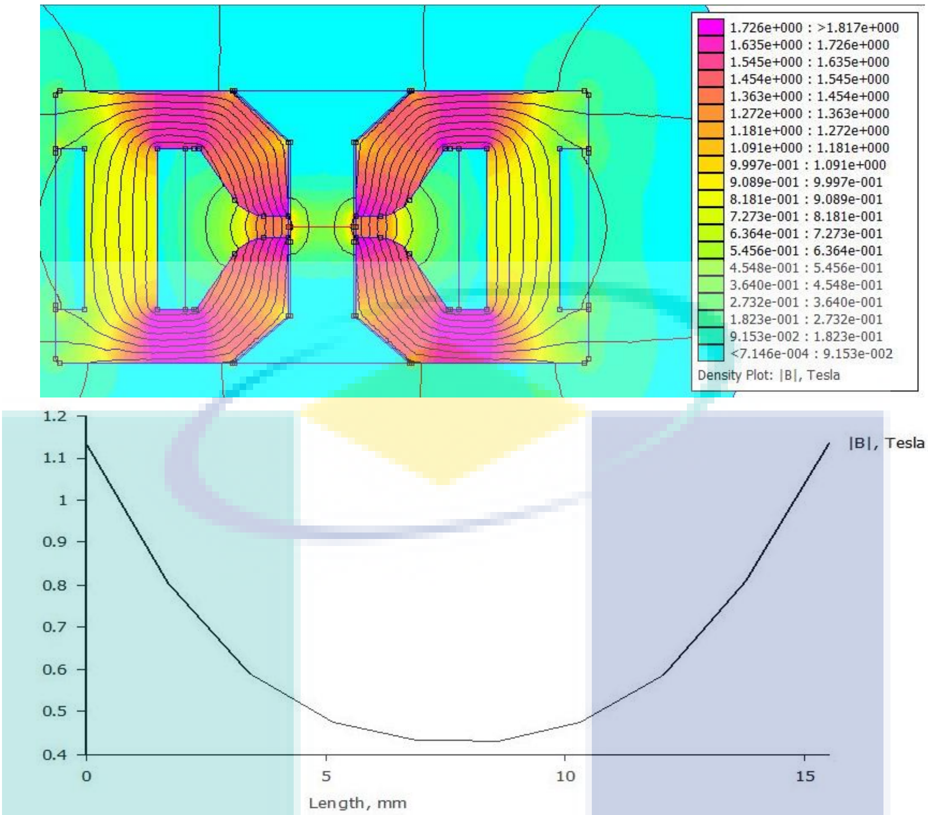

Figure 4.12 Magnetic flux distribution for sample 4

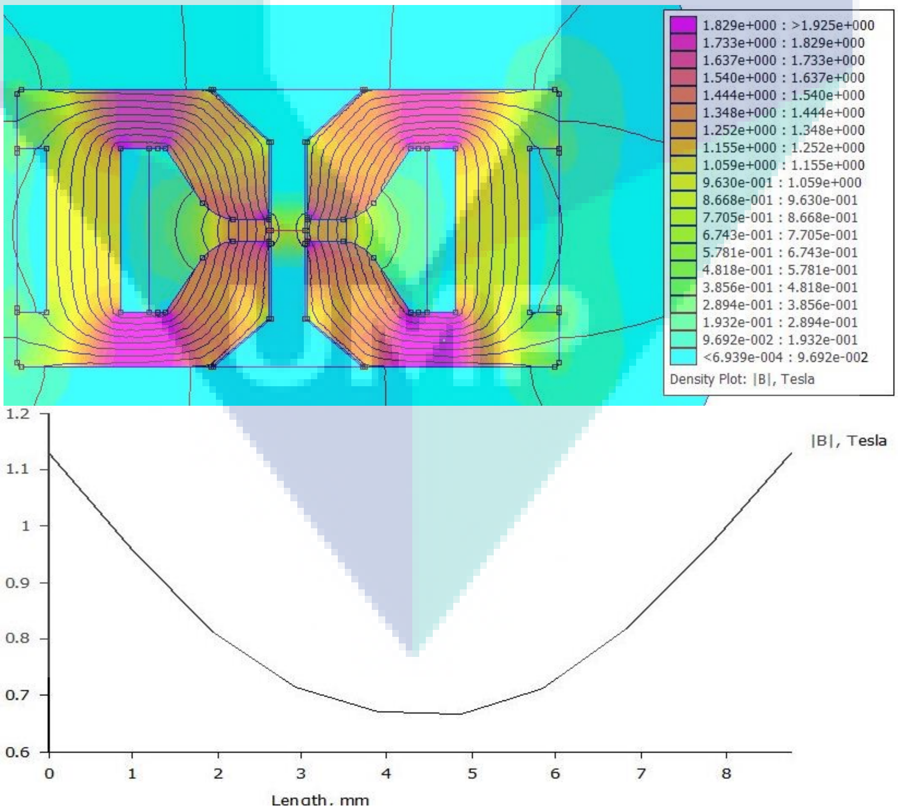

Figure 4.13 Magnetic flux distribution for sample 6

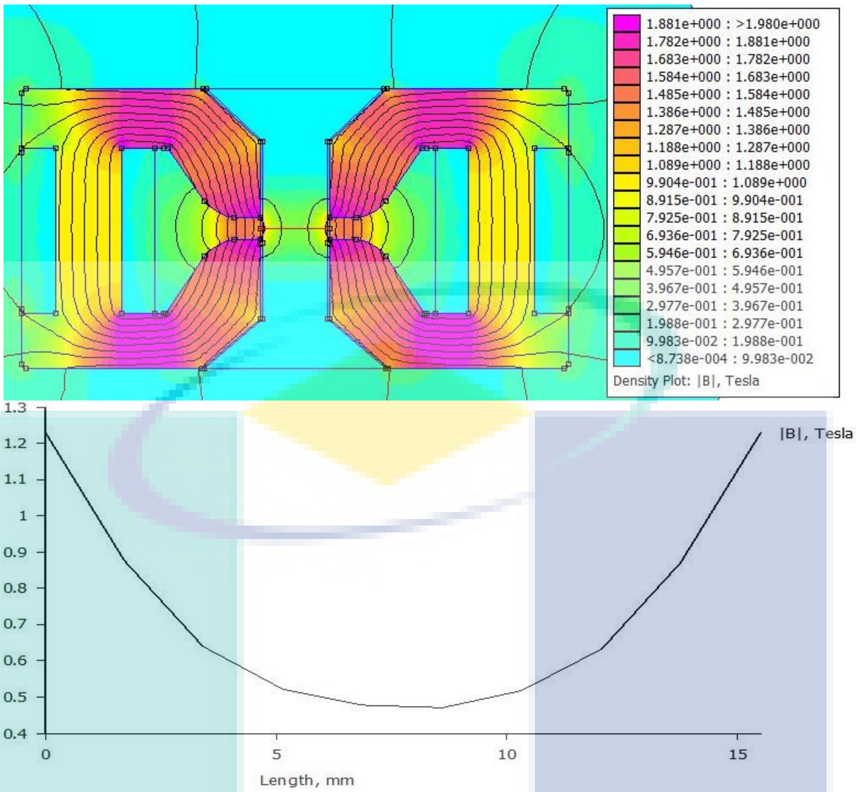

Figure 4.14 Magnetic flux distribution for sample 7

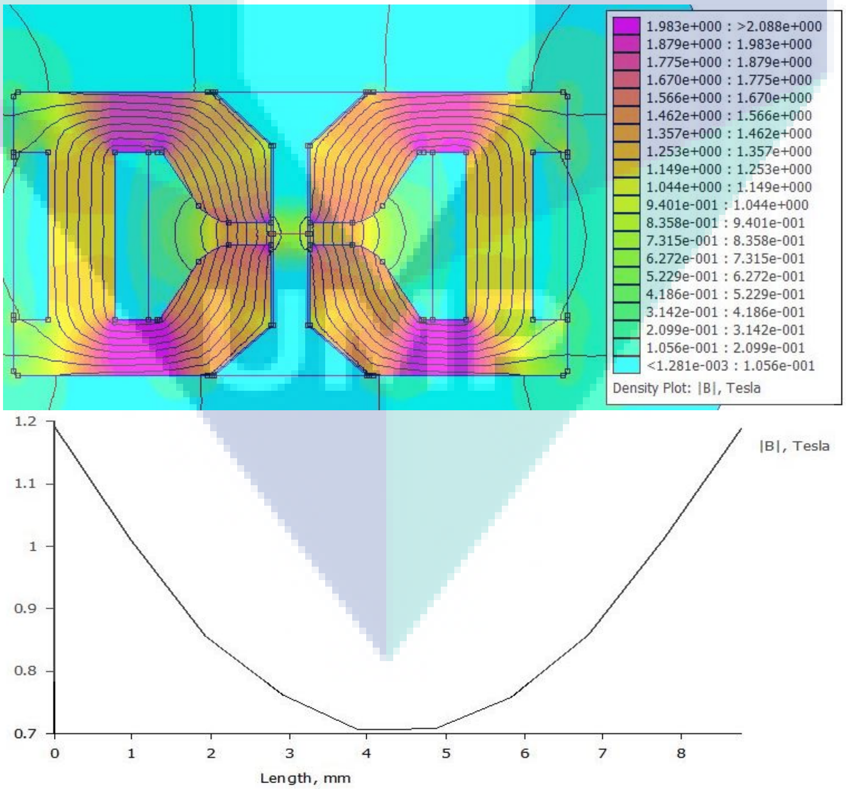

Figure 4.15 Magnetic flux distribution for sample 8

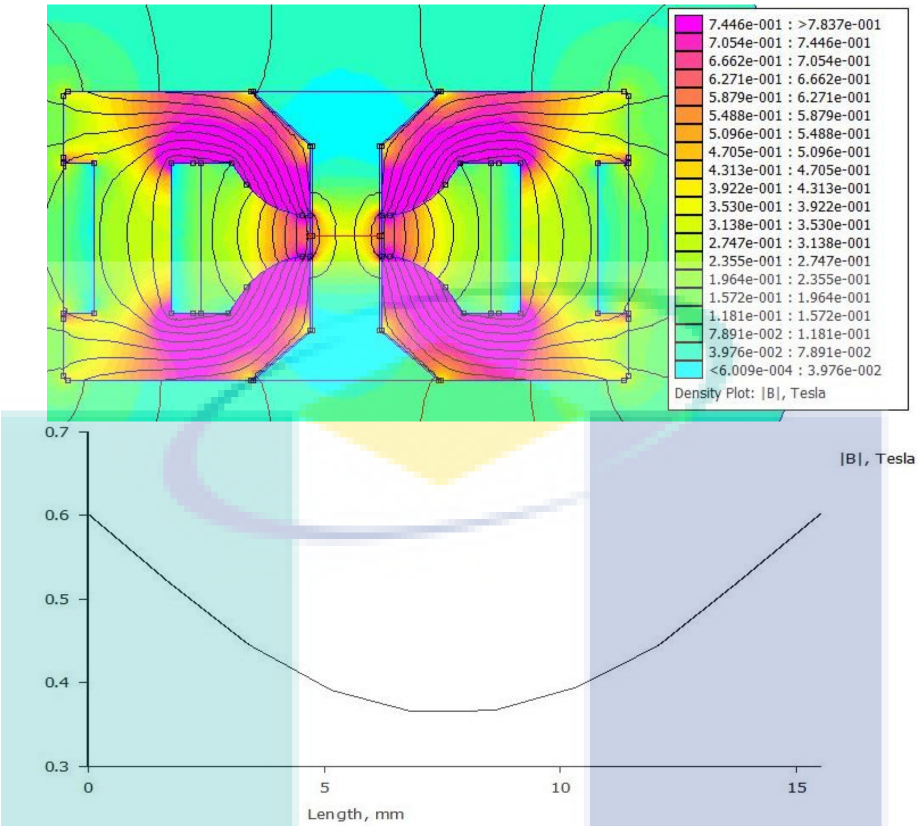

Figure 4.16 Magnetic flux distribution for sample 9

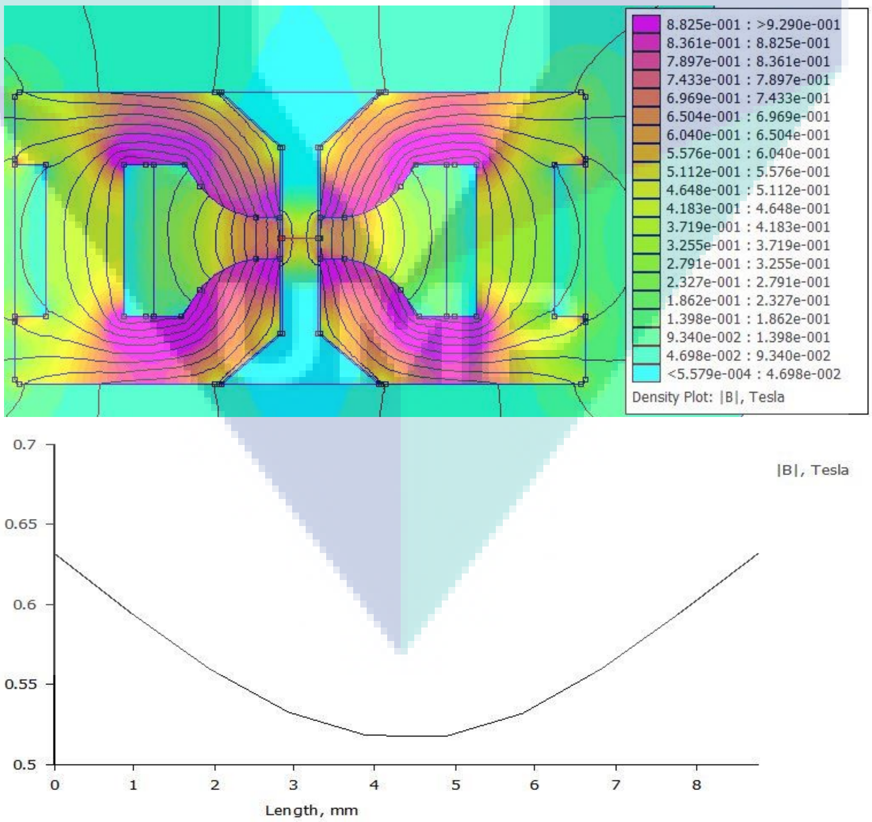

Figure 4.17 Magnetic flux distribution for sample 10

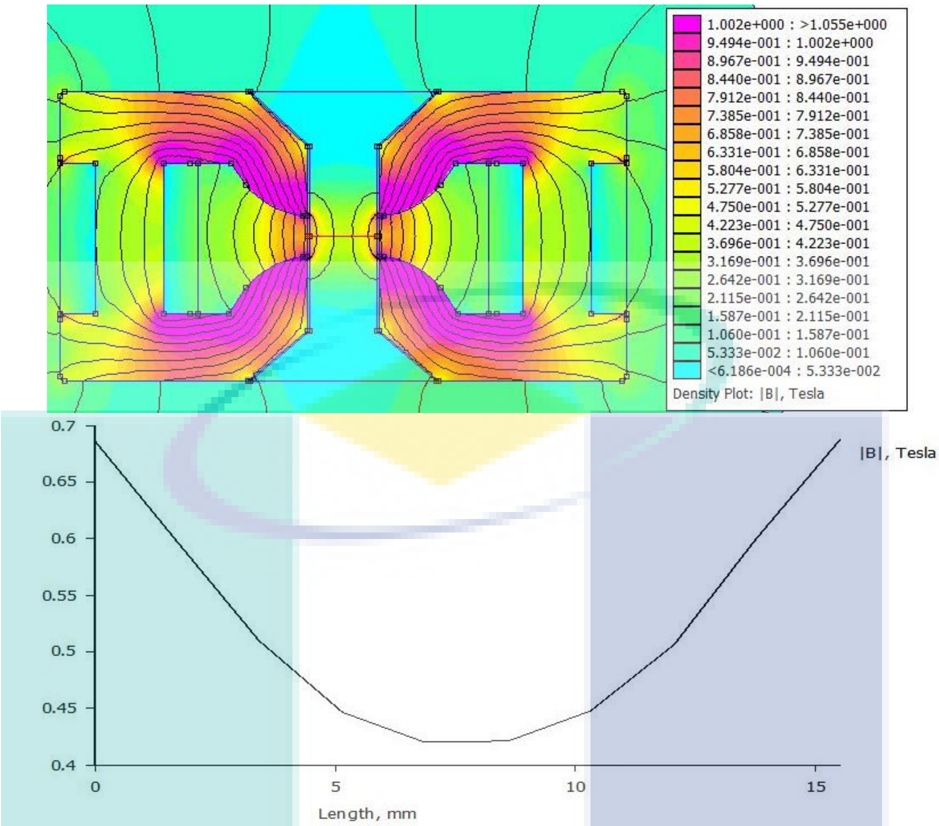

Figure 4.18 Magnetic flux distribution for sample 11

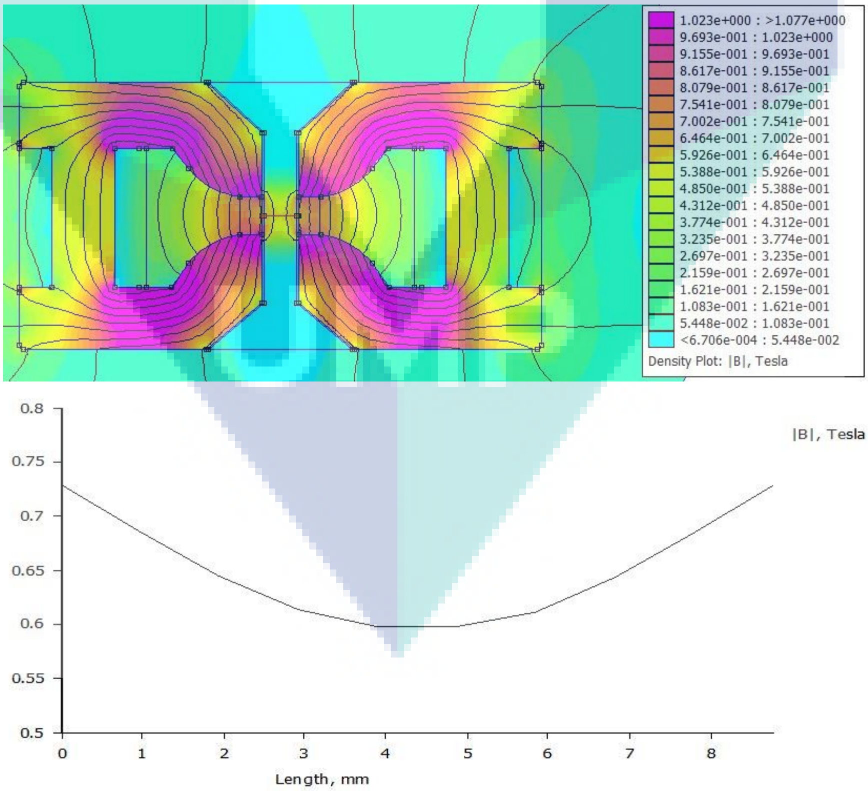

Figure 4.19 Magnetic flux distribution for sample 12

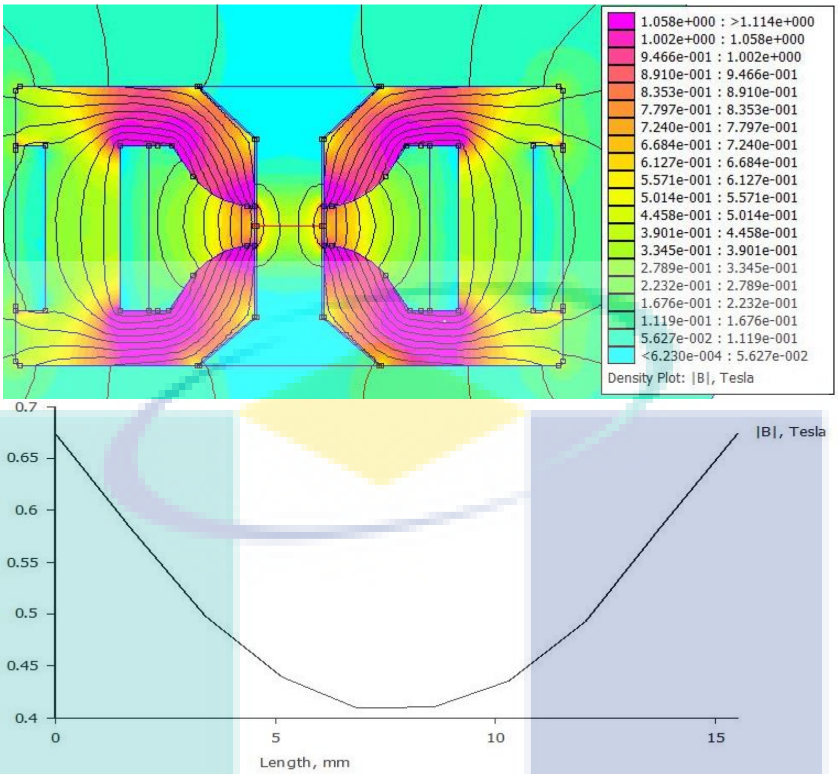

Figure 4.20 Magnetic flux distribution for sample 13

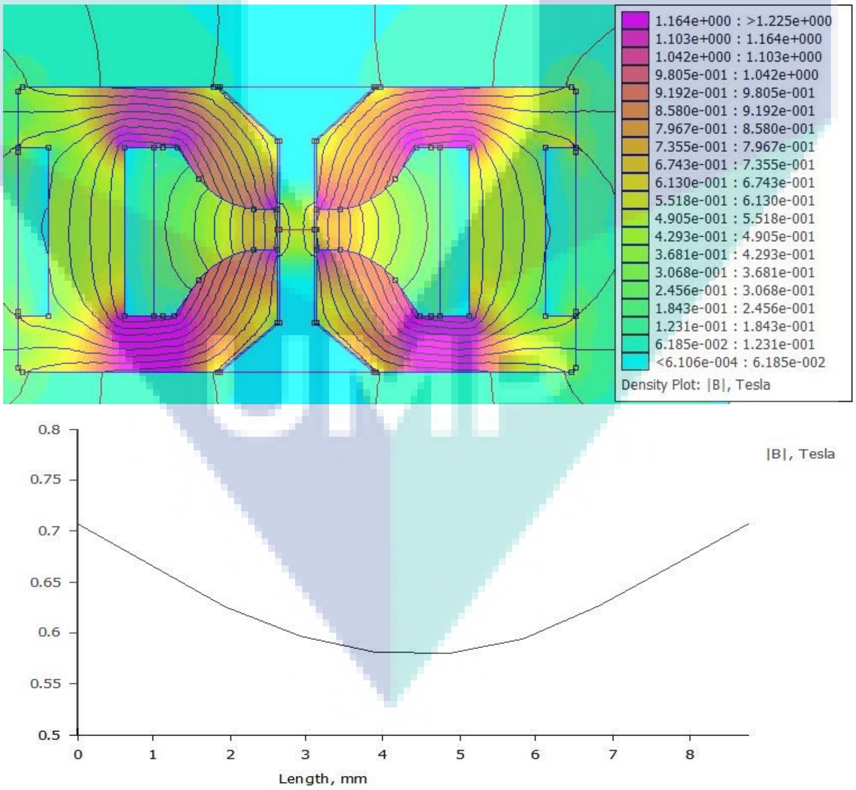

Figure 4.21 Magnetic flux distribution for sample 14

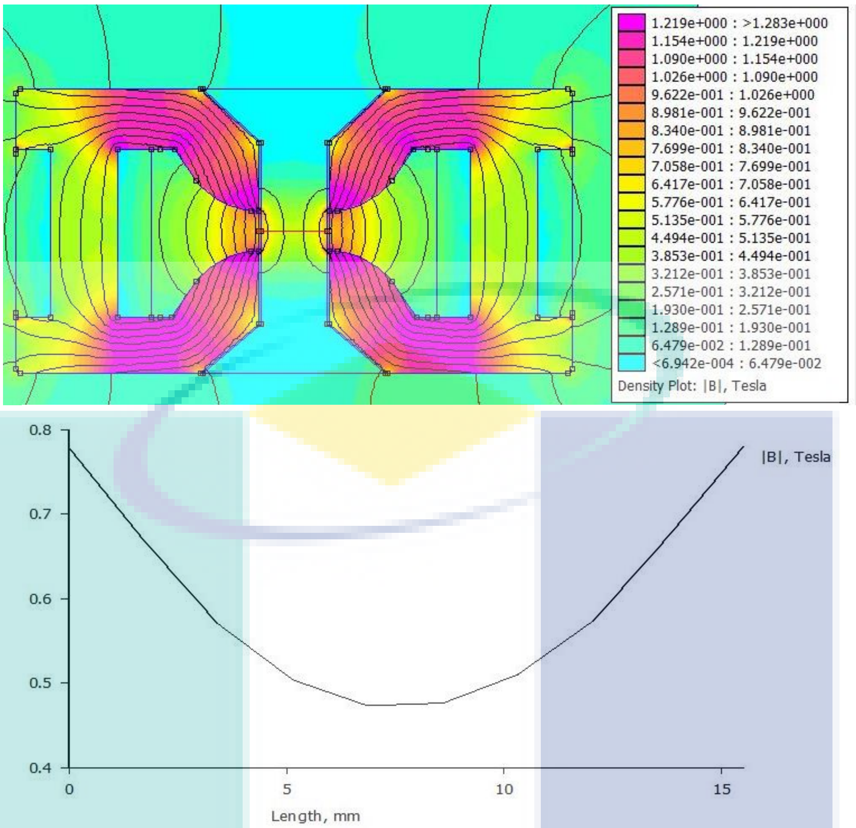

Figure 4.22 Magnetic flux distribution for sample 15

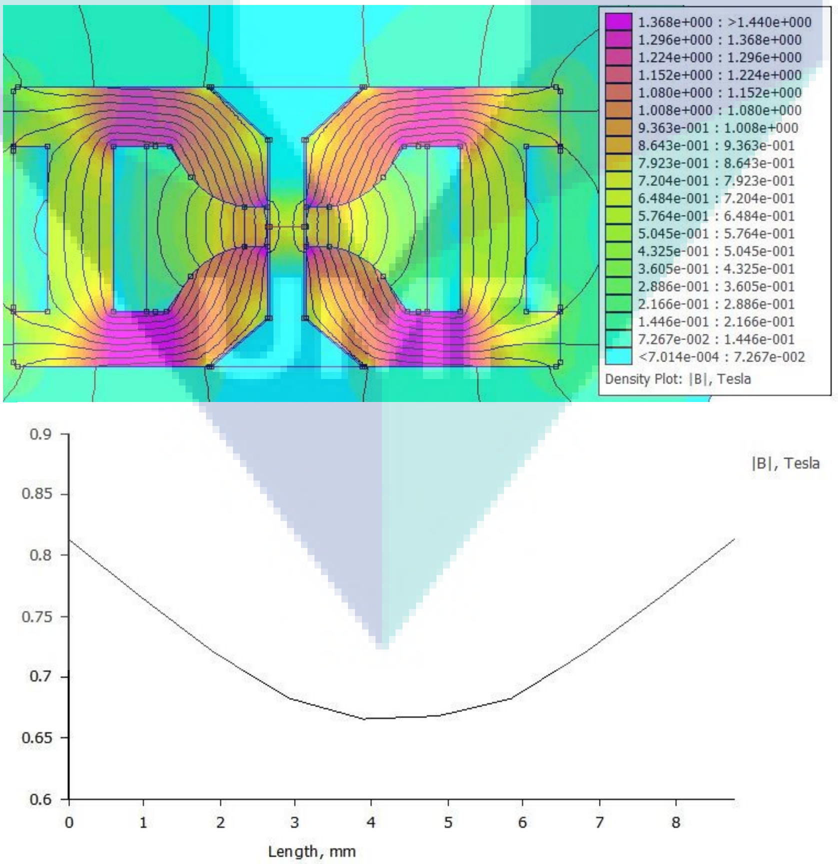

Figure 4.23 Magnetic flux distribution for sample 16

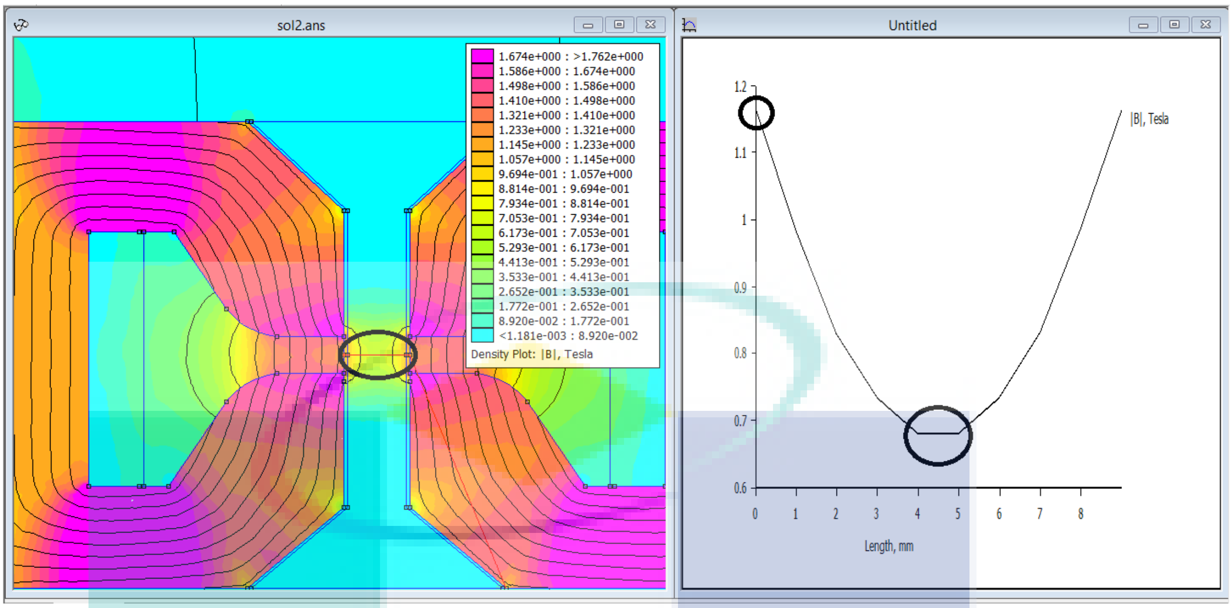

Figure 4.24 The result obtained with the magnitude of flux density graph

Figure 4.24 shows the result of simulation and the magnitude of flux intensity graph. The black circle is the region where we want to measure the magnitude of flux intensity. The length of gap for MR fluid to flow in this simulation is 8 mm. We get is about 9.27×10^5 Amp/m at 0 mm. When it reach at 4.44 mm the reading drop to 5.41×10^5 Amp/m, and it keeps increasing back to 9.27×10^5 Amp/m when it reach at 8 mm.

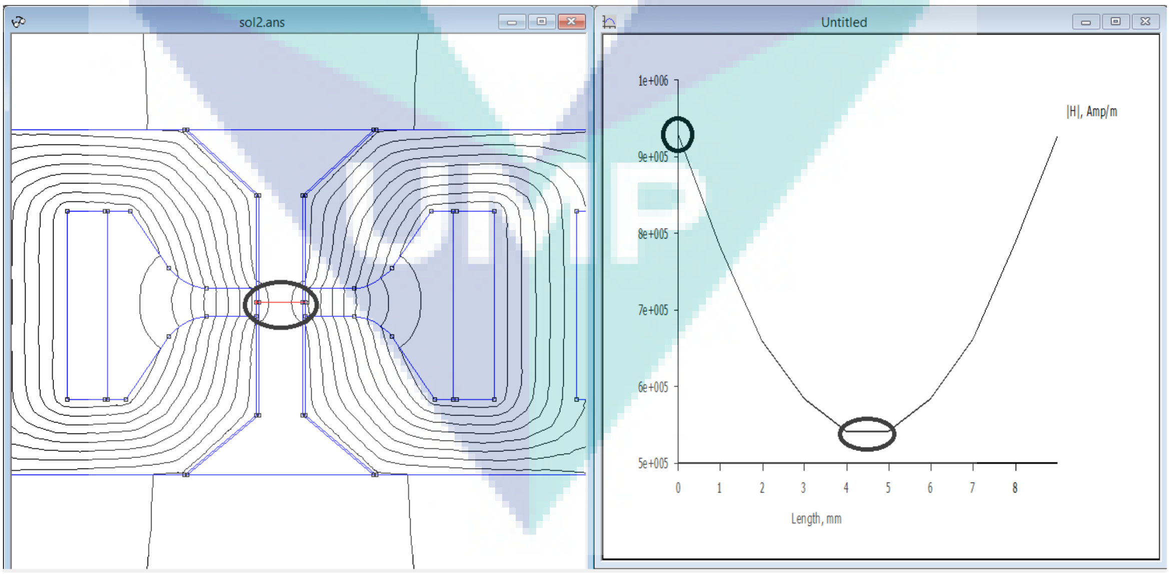

Figure 4.25 The result of flux density along the cross-section of the chocked area.

The size of the parameter and the value of the maximum and minimum magnetic flux are collected from simulation using FEMM software are key in the Expert Design software. The simulation has been run for 16 times.

4.2.2 ANOVA and optimization

Analised finite element simulation result of all geometrical size combination is shown in table 4.1. The minimum magnetic flux ranges from 0.36 T to 0.7, while the maximum magnetic flux ranges from 0.58 to 1.12 T. The ratio of maximum and minimum magnetic flux was ranged from 1.2 to 2.5. Ratio near to 1 indicates stable magnetic flux at the choking region. While the large value of the ratio indicates irregularity of the magnetic field at the choking area.

Table 4.1 Geometry of each parameter

Sample No.	A: Outer Width (mm)	B: Coil Width (mm)	C: Core Length (mm)	D: Pinch Gap (mm)	Min Magnetic Flux (Tesla)	Max Magnetic Flux (Tesla)	Ratio (Min, Max)
1	57.00	6.50	37.00	5.00	0.46	1.08	2.3
2	54.00	7.50	37.00	9.00	0.47	0.75	1.6
3	54.00	6.50	33.0	5.00	0.39	0.97	2.5
4	57.00	7.50	33.00	9.00	0.6	0.71	1.2
5	57.00	6.50	37.00	9.00	0.58	0.69	1.2
6	54.00	6.50	33.00	9.00	0.36	0.58	1.6
7	57.00	7.50	37.00	5.00	0.7	1.1	1.6
8	54.00	7.50	37.00	5.00	0.47	1.12	2.4
9	54.00	7.50	33.00	9.00	0.42	0.66	1.6
10	54.00	6.50	37.00	9.00	0.41	0.65	1.6
11	57.00	7.50	33.00	5.00	0.68	1.09	1.6
12	57.00	6.50	33.00	9.00	0.6	0.71	1.2
13	54.00	6.50	37.00	5.00	0.43	1.04	2.4
14	54.00	7.50	33.00	5.00	0.46	1.08	2.3
15	57.00	6.50	33.00	5.00	0.63	0.99	1.6
16	57.00	7.50	37.00	9.00	0.67	0.79	1.2

Optimization results

Table 4.2 shows optimization criteria where all the factors are defined as 'in range'. The response of the MR pinched mode parameter defined the equally in maximize. All factors and responses are set to be equal importance respectively.

Table 4.2 Optimization of lower and upper limit of MR pinched mode parameter

Factors And Responses	Lower Limit	Upper Limit	Criteria	
			Goal	Importance
Outer Width	54	57	in range	3
Coil Width	6.5	7.5	in range	3
Core Length	33	37	in range	3
Pinch Gap	5	9	in range	3
Min Magnetic Flux	0.36	0.7	maximize	5
Max Magnetic Flux	0.58	1.12	maximize	5

The predicted optimal of the geometry parameter values are shown in Table 4.3. There are thirty solutions where desirability ranging between 0.687 until 0.874. Solutions number 1 (S1) has been selected as the most preferable solution who possessed the desirability value close to 1. It is clearly shown that pinch gap plays an important role in the formation of magnetic flux due to the equal value for all solutions. This is further proven by figure 4.2 and 4.3. Furthermore, the core length were suspected as no effect mechanism in contribution of the magnetic flux value. The inconstant and variety range of core length parameter contribute to no effect status of magnetic flux.

Table 4.3 Predicted the optimal geometry parameter for minimum and maximum magnetic flux.

Number	Outer Width	Coil Width	Core Length*	Pinch Gap	Min Magnetic Flux	Max Magnetic Flux	Desirability
1	57	7.5	34.75	5	0.65	1.06	0.874
2	56.98	7.5	33.34	5	0.65	1.06	0.872
13	57	7.48	33	5	0.65	1.06	0.871
14	56.96	7.5	36.71	5	0.65	1.06	0.871
19	57	7.34	33.01	5	0.64	1.06	0.856
25	57	6.95	33.05	5	0.61	1.06	0.809

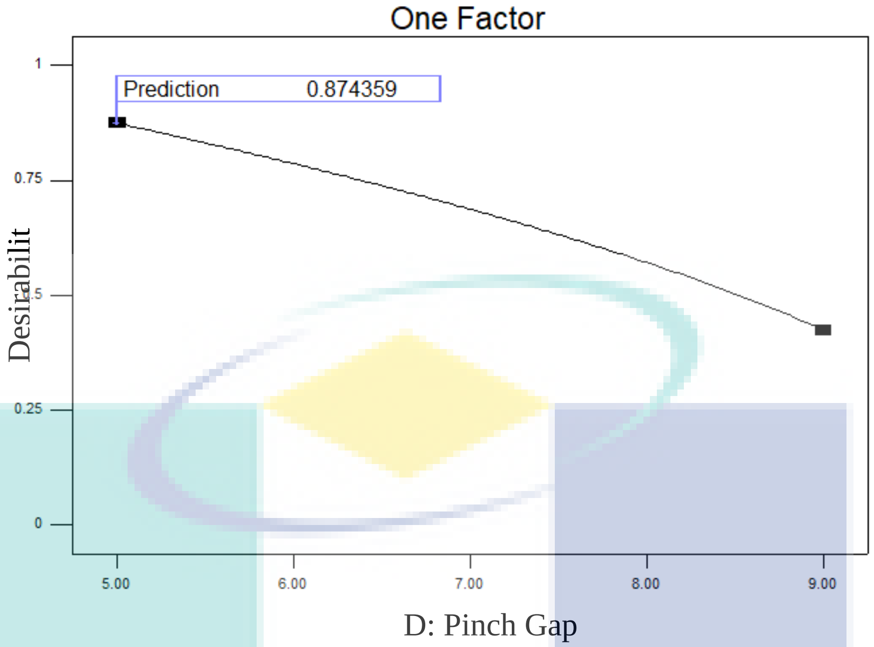

Figure 4.26 Optimization graph on the desirability

Figure 4.26 the desirability graph of the geometry parameter for MR pinched mode valve. The goal of this desirability optimization is to find a good set of conditions that will meet all the goals and optimum value. Well known, the main part of this study is to get the best magnetic field in the effective area. From the graph, the desirability of magnetic flux in this study is 0.874359 at the lowest pinch gap size, which the objective of the desirability limit should not more than one. The optimum pinched gap size has been shown in figure 4.26. Hence, the desirability of the magnetic flux is in range 0 to 0.874359.

Figure 4.27 shows one factor graph on maximum magnetic flux versus pinch gap. This is one of the scope research to be followed to examine which parameters have a great impact on the magnetic fields at the effective area. The result revealed that the pinch gap parameter relevant to be one of factor whose obey the pinch mode concept. The lower the pinch gap value, the higher the magnetic flux value produce. Similarly, the situation was proved and supported by (Goncalves and Carlson 2009) in their study. The results shows the pinch gap occurs at level 5 mm to 9 mm. Therefore, it can be concluded that, the best parameter of pinch gap to be used is 5 mm since the level of pinch gap occurs at this range. Meanwhile the prediction value of maximum and minimum magnetic flux is 1.05875 and 0.6925 respectively.

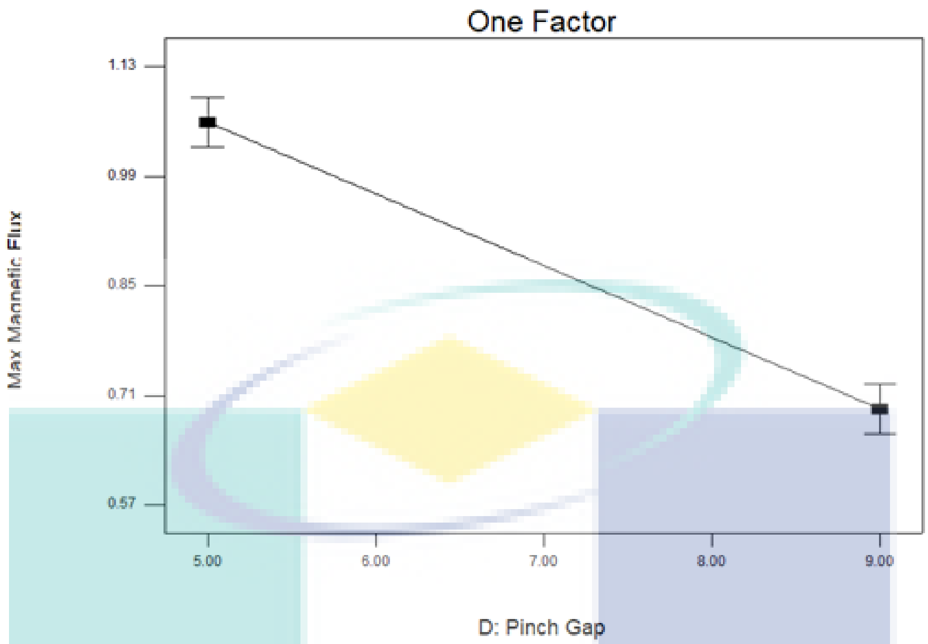

Figure 4.27 Magnetic Flux at the maximum and minimum of pinch gap size

Table 4.4 Final geometry of MR pinched mode valve

Geometry Parameters	Outer Width,	Coil Width,	Core Length,	Pinch Gap,	Min. Magnetic Flux	Max, Magnetic Flux	Desirability, Tesla
	57.00	7.50	33.80	5.00	0.653124	1.05875	0.874

There were 29 solutions of geometry optimization. This one has been selected as the final parameter before the instrument have been fabricated. All the final parameter has been analysed by using FEMM software.

4.3 The developed prototype of the pinched mode valve

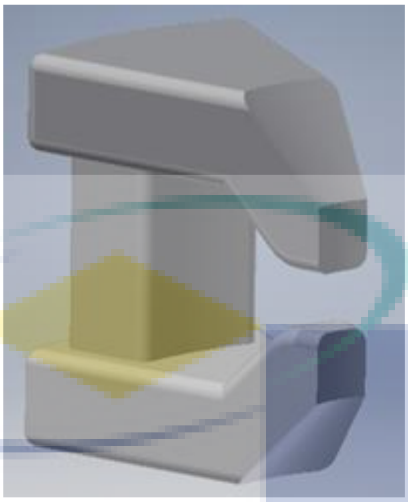

Figure 4.28 Isometric view of new C-magnet of MR pinched mode valve

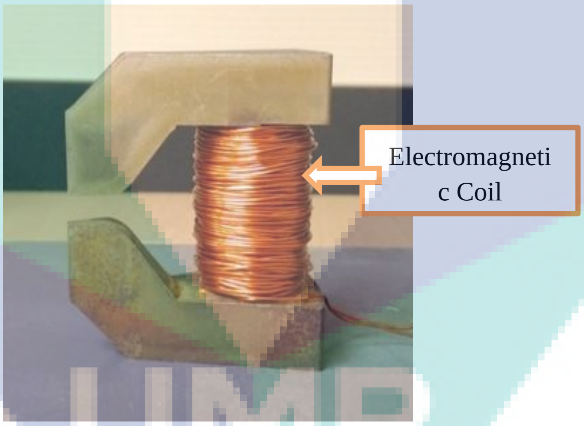

Figure 4.29 Wined magnet wire on 'C' electromagnetic core.

The magnetic field occur because of the presence of electric supply, current and voltage through the coil. In this study, the electromagnetic coil is wounded around the core. The magnetic field is guided through the pinch gap parallel to the fluid flow.

All the parameter geometry and materials have been considered for the evaluation. For the geometry calculation, it had been done the trial and error operations to find out the value of turns coil in order to provide the field strength.

4.3.1 Magnetic flux analysis

In this section, it describes the simulation to obtain the optimum value for magnetic flux at the effective area. Then, it directly shows the effect of the magnetic field strength on the pressure drop. There has been some changes in the design section to achieve a robust magnetic flux which is not limit then the commercial MRF 132DG, 0.78 Tesla.

Table 4.5 The simulation data of new fabricated MR Pinched mode valve

Length (mm)	Magnetic Field (Tesla)
0.00	0.08
0.90	0.07
1.79	0.06
2.69	0.05
3.58	0.05
4.48	0.05
5.37	0.05
6.27	0.06
7.16	0.07
8.06	0.08

In detail, the current outer length of magnet is 60 mm and its outer width is 57 mm. The core gap is 5 mm, core length is 34.3 mm and the coil width is 7.5 mm. The core was made by magnetic material. The copper wire have been selected in supplying the current which 1.4 A in control. It also incorporates 320 turns of 0.644 mm diameter to influence the magnetic field distribution in flow gap. The effective area of a channel is 8 mm.

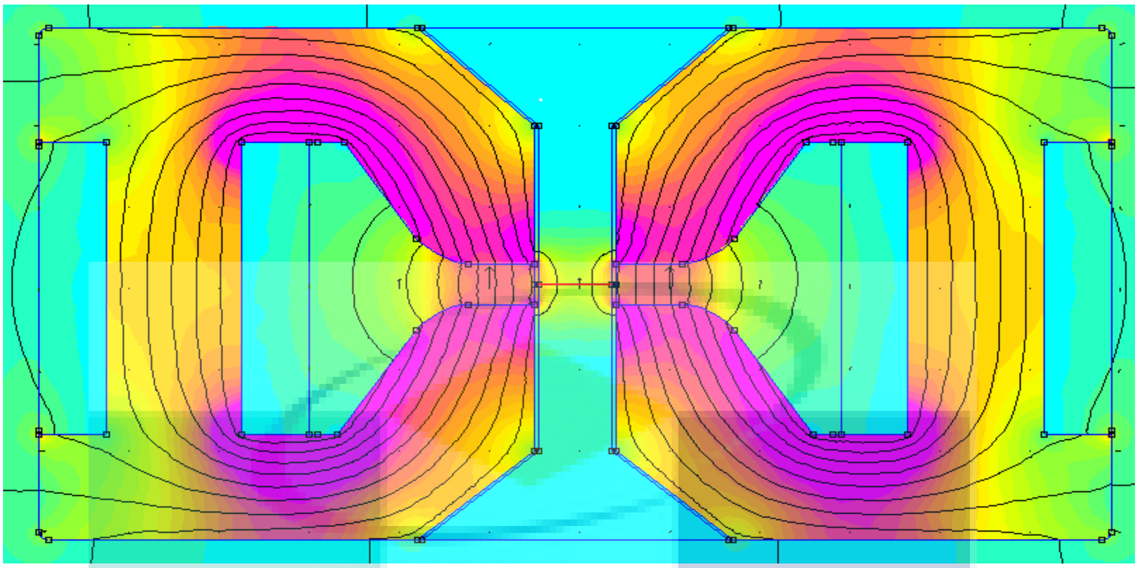

Figure 4.30 Plots of reference figure of valve assembly for B (Tesla) and H (A/m)

Figure 4.30 shows the 2D plots of simulated magnetic flux of magnetic field density (B) and the length. There is clearly shown the magnetic field distribution around an effective area (black line). The magnetic test was carried out by applying the various current. The magnetic flux value at the effective area as per shown in Figure 4.5. In theory, the maximum current value of the 22 AWG wire is 3A (Ltd.). However, in actual there are some errors during the experimental session. The ability of power supply to support is only 1.4 A with 10 V. This thing happens because the resistance value is not same as for the fabricated C-magnet. After being investigated, this inequality may be due to damage on the electromagnetic coil during the winding work done. Because of this consequences, it affects the magnetic flux value during the experimental, as shown in Figure 4.31. There shows the actual reading value of magnetic flux in the effective area by using FEMM analysis. The maximum of the magnetic flux is 0.08 Tesla and the minimum was 0.05 Tesla

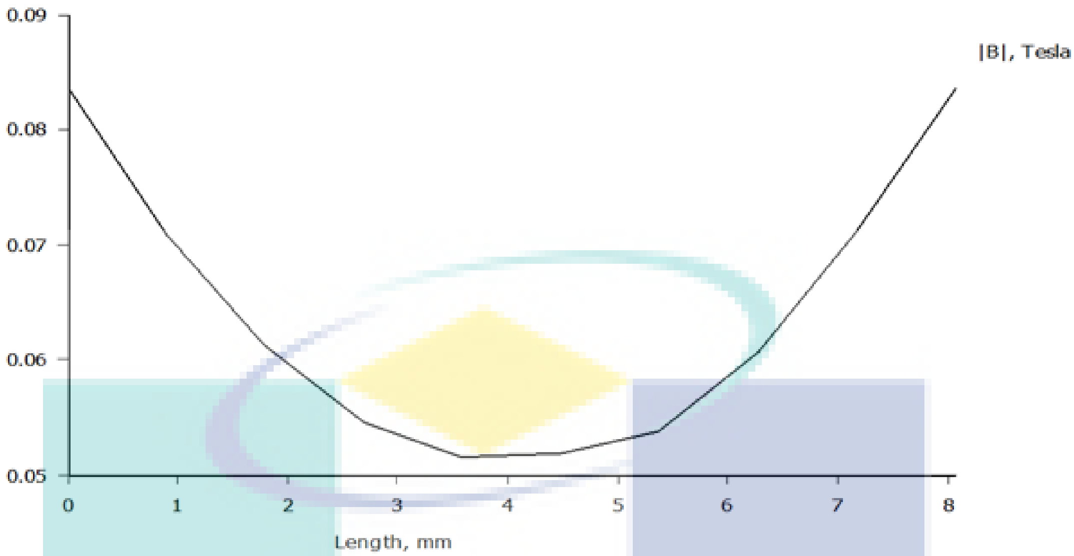

Figure 4.31 FEMM magnetic flux density of B in the effective's area

4.3.2 Experimental Results

In this study, the pressure drop depends on the magnetic fluid flow where it is parallel towards the flow rate of the MR fluid. For the final result of this study, a number of electromagnetic coil and the geometry of core of new MR pinched mode valve have been calculate many times in order to evaluate better performance.

Figure 4.32 shows the relationship between magnetic flux and current. The strength of magnetic field is directly proportional to the current flow. Once the current is apply, a magnetic field around the conductor will be produced. This indicates the validity of the value obtained during the experimental. As seen from the figure, the high of the current supply, the high of magnetic flux. Unfortunately, there is a fluctuation occur at the 0.0438 Tesla, 1.3 A of result. This has been discussed in figure 4.31 result.

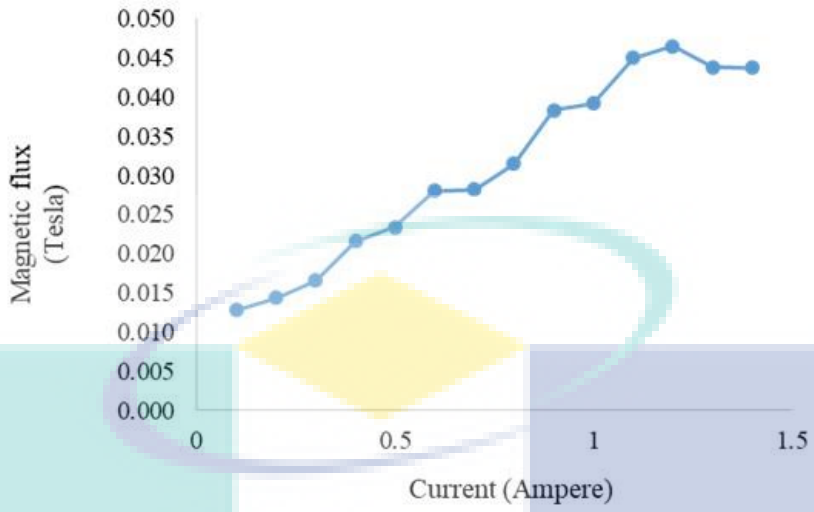

Figure 4.32 The magnetic flux at various current supply.

4.4 Performance of the pinched mode valve

For the result between pressure and current supply, it shows the same effect on graph formation, since the range of current supply is constant as shown in Figure 4.33. Hence, the higher the current supply, the higher the pressure value will be produced. The pressure drop of this experiment was determined by the differentiation between inlet and outlet pressure as in equation 4.0.

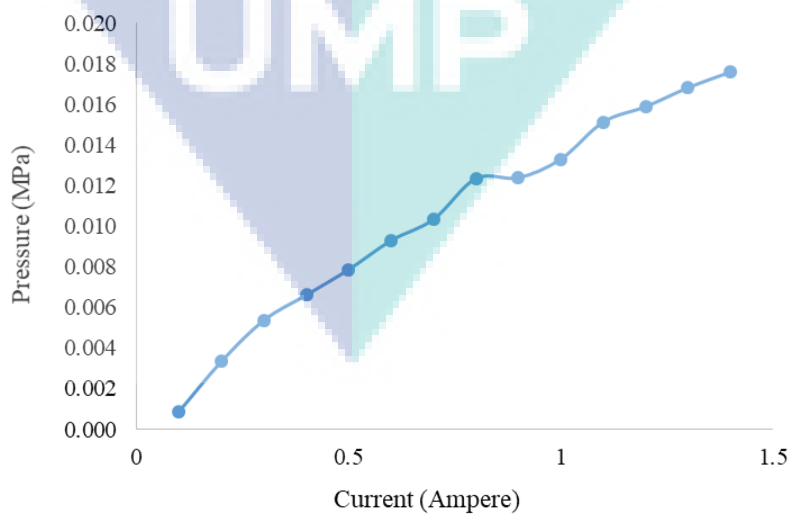

Figure 4.33 Pressure drop at various current input

$$\Delta P = P_{in} - P_{out} \quad 4.0$$

The main factor of pressure drop in the valve because of the fluid velocity and viscosity. Pressure drop happens when the fluid flow input and output of the valve give the experience of some resistances to flow due to the friction, whether because of internal friction of fluid or friction between fluid and the fluid flow channel.(Abd Fatah, Mazlan et al. 2015)

Theoretically, the inlet pressure value can be determined by using the suitable formula as shown in equation 4.1 and require a bit manual calculation to obtain the value. Meanwhile, the area of cylinder can be determined by using the mathematical formula as per equation 4.2.

However, in this experiment, the value of inlet pressure automatically producing by Universal Tensile Machine (UTM) when the load has been applied on the new MRF pinched mode device. The results have been plotted as in Figure 4.7.

$$P_{in} = \frac{F}{A_{cyl}} \quad 4.1$$

$$A_{cyl=} \text{ Area of cylinder} = 2\pi r^2 + 2\pi rh \quad 4.2$$

In the other hand, outlet pressure (P_{out}) value is set as zero that equal to the atmosphere ($P_{out} = P_{atm} = 0$).

Based on Figure 4.34, it can be interpreted that, in order to push the MRF fluid out of the channel, it requires a different pressure. The higher the pressure value, the farther the fluid needs to be pushed out. This is due to the friction between the fluid in the channel and viscosity of fluid.

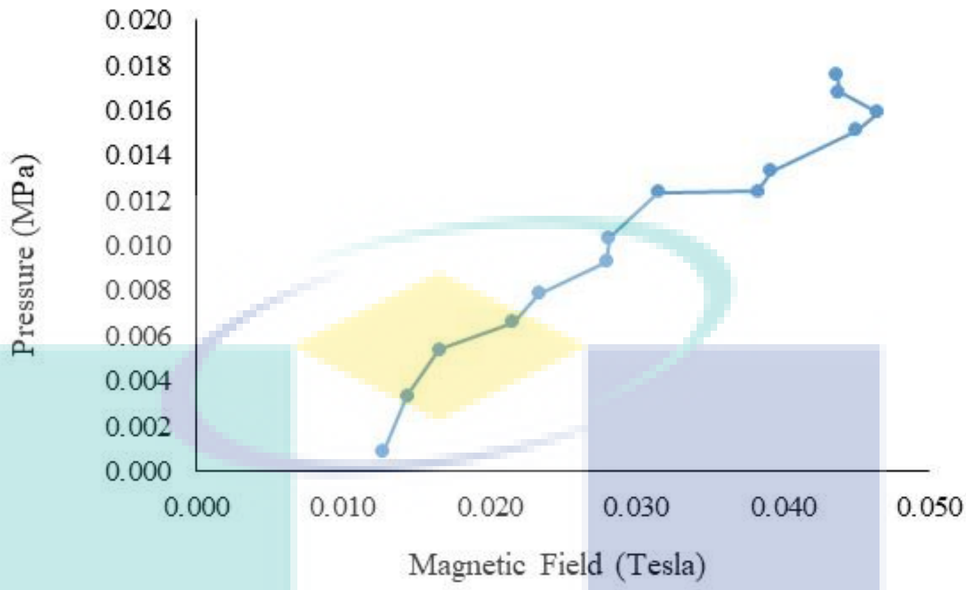

Figure 4.34 Graph Magnetic field versus pressure.

The pressure drop is proportional to the flow rate. This situation is similar to what applies in the absence of a magnetic field. Based on figure 4.34, it shows the magnetic field versus pressure during the presence of magnetic field. When the high pressure have been applied, the high magnetic field also being produce. However, this relationship is not much significant. The pressure drop increases only 0.2 % meanwhile magnetic field shows up to 0.5 %.

Based on the experiment results on magnetic field distribution, the mechanisms between electromagnetic and fluid channel were contradictory which may affect the energy transfer on fluid flow and viscosity behaviour.

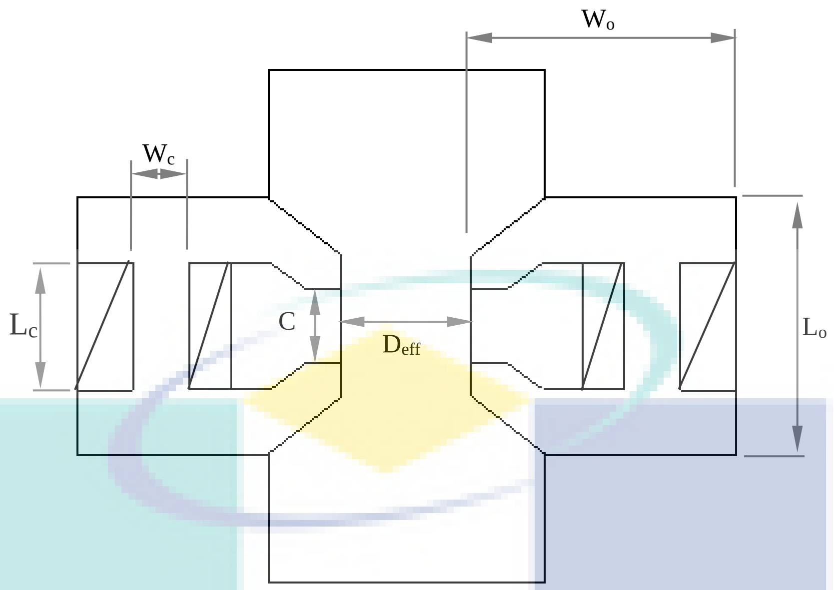

Figure 4.35 Illustrated of 2D plannar model of final concept MR pinched mode valve

In detail, the current outer length of magnet is 64 mm and its outer width is 56 mm. The core gap is 7mm, core length is 35 mm and the coil width is 6.5 mm. The magnet material is pure iron and the channel material is stainless steel. The copper wire have been selected in supplying a current which 3A in control. It also incorporates 1299 turns of 0.644 mm diameter to influence the magnetic field distribution in flow gap. The effective area of a channel is 12 mm.

The magnetic field distribution inside of MRF pinched mode valve was simulated by using Finite Element Method (FEMM) software. A two-dimensional model of MR pinched mode mechanism have been designed with supported of boundary conditions, material properties and electromagnetic activation current.

Figure 4.36 shows the basis for planar view of two-dimensional model developed in FEMM. The obtained results for the red circle area were shown in figure 36.

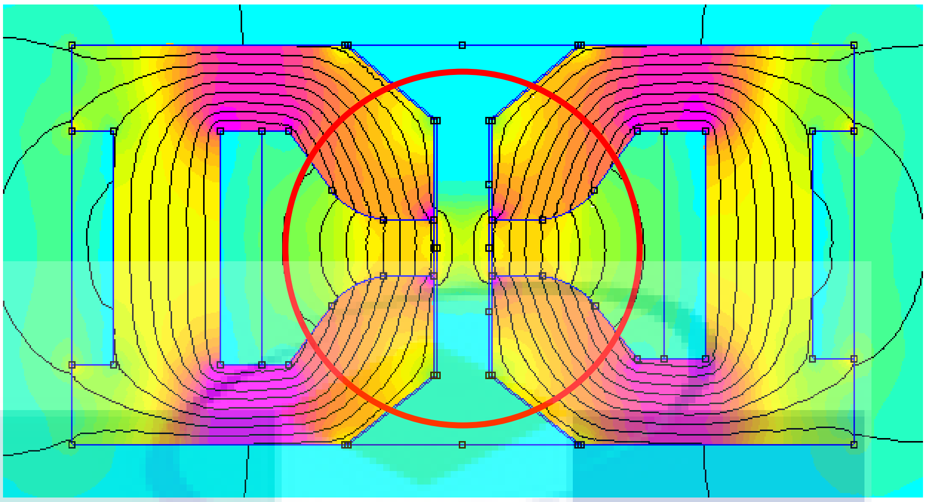

Figure 4.36 2D asymmetric of FEMM software

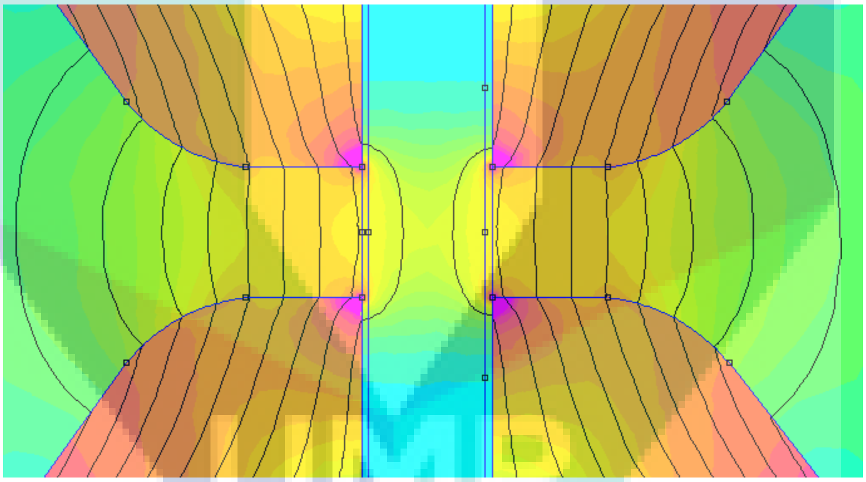

Figure 4.37 Middle line of choked area (A-B) and channel (red line)

The flux density variation in gap area is shown in figure 4.37. In this figure, ‘A’ denotes as the inlet flow and ‘B’ is the outlet flow of material in the channel. The results were computed for the coil ampere turns (NI) range 3897 AT in figure 5d.

The red line area also known as an effective area of magnetic field distribution where at this point the choking effect happen. The red line indicate the flux density which are varies from approximate 0.49T to 0.8T, illustrated in Figure 4.38

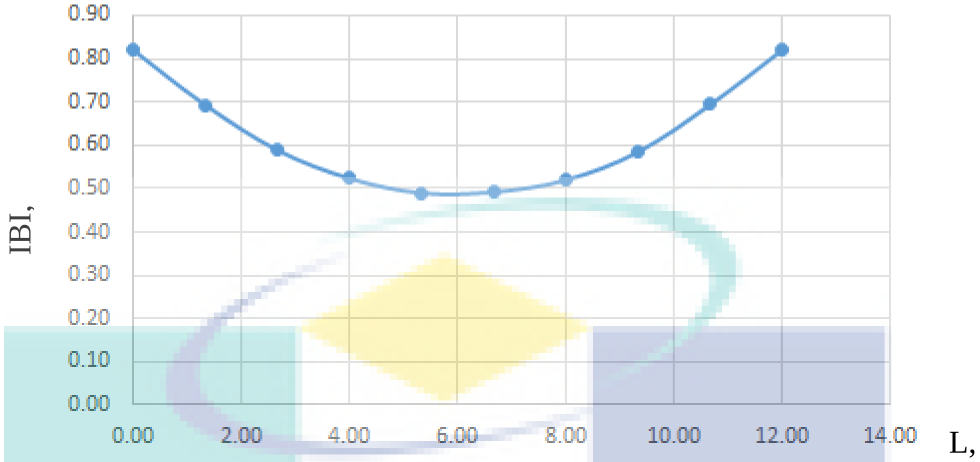

Figure 4.38 Flux density variation at the effective area with 3A current supply

CHAPTER 5

CONCLUSION

5.1 Conclusion

The new MR pinched mode valve have been successfully developed. It has the potential to be used in the automotive and civil structure suspension system. Specifically, three main conclusions from this study are spelt as followed:

1. Electromagnetic field distribution was simulated using the finite element method. The simulation indicates geometrical size and shape change the magnetic field distribution at the choking area. Tailoring the geometry allows designing magnetic distribution strength and pattern that suitable for pinched mode valve.

2. The prototype of the pinched mode magnetorheological valve was produced and tested. The design involves concept improvement and optimised geometrical size. Based on the final design, MR pinched mode valve consist of three main components. There are non-magnetic, magnetic materials and electromagnetic circuit.

3. The fabricated MR pinched mode magnetorheological valve went through a pressure test to evaluate the performance. The pressure drop increased with the increases in the magnetic strength. The coil winding and current supply be the main important character in the formation of the magnetic field.

5.2 Contribution to the study.

In this thesis, the DOE and the optimization of the geometry parameter in this study can be used for high-pressure resistance application. The new MR pinched mode valve for high-pressure resistance was successfully developed.

The highest 0.044 Tesla of the magnetic field at 0.018 MPa pressure can be used as a reference data for high-pressure resistance application of MR pinched mode valve.

In the other hand, each of the geometry parameters has a significant effect on the magnetic field distribution so as the MR fluid behaviour.

5.3 Recommendation for future works

There are few points that can be jot down in order to improve the current design and method use for this study in the future works:

i. Determine the design geometry parameters of new MR pinched mode valve size for specific applications only.
ii. Fabricate more electromagnetic core so that the effect of magnetic field during pressure drop can be identify well.
iii. Modified the winding coil by using proper winding tools.
iv. Preparing and pay more attention on the material selection of magnetic device so as the magnetic field distribution can be determine wisely as per simulation analysis.

REFERENCES

Ahamed, T. I., Sundarrajan, R., Prasaath, G., & Raviraj, V. (2014). Implementation of magneto-rheological dampers in bumpers of automobiles for reducing impacts during accidents. Procedia Engineering, 97(1), 1220-1226.

Ashtiani, M., Hashemabadi, S. H., & Ghaffari, A. (2015). A review on the magnetorheological fluid preparation and stabilization. Journal of Magnetism and Magnetic Materials, 374, 716-730. doi:https://doi.org/10.1016/j.jmmm.2014.09.020

Asri, M. Z. (2016). Magnetic Field Simulation of Pinch Mode Magnetorheological Fluid Valve. Universiti Malaysia Pahang,

Baranwal, D., & Deshmukh, T. S. (2012). MR-Fluid Technology and Its Application-A Review. International Journal of Emerging Technology and Advanced Engineering, 2, 563-569.

Bica, I., Liu, Y. D., & Choi, H. J. (2013). Physical characteristics of magnetorheological suspensions and their applications. Journal of Industrial and Engineering Chemistry, 19(2), 394-406. doi:https://doi.org/10.1016/j.jiec.2012.10.008

Boelter, R., & Janocha, H. (1997). Design rules for MR fluid actuators in different working modes (Vol. 3045): SPIE.

Carlson, J. D., & Jolly, M. R. (2000). MR fluid, foam and elastomer devices. Mechatronics, 10(4), 555-569. doi:https://doi.org/10.1016/S0957-4158(99)00064-1

Choi, H. J., Jang, I. B., Lee, J. Y., Pich, A., Bhattacharya, S., & Adler, H. (2005). Magnetorheology of synthesized core-shell structured nanoparticle. IEEE Transactions on Magnetics, 41(10), 3448-3450. doi:10.1109/TMAG.2005.855197

Daniel, G., Yoan, C., Zoltan, P., & Yves, P. (2014, 8-11 July 2014). Bingham-papanastasiou and approximate parallel models comparison for the design of magneto-rheological valves. Paper presented at the 2014 IEEE/ASME International Conference on Advanced Intelligent Mechatronics.

Dimock, G. A., Yoo, J.-H., & Wereley, N. M. (2002). Quasi-steady Bingham biplastic analysis of electrorheological and magnetorheological dampers. Journal of intelligent material systems and structures, 13(9), 549-559.

Dohmen, E., Borin, D., & Zubarev, A. (2017). Magnetic field angle dependent hysteresis of a magnetorheological suspension. Journal of Magnetism and Magnetic Materials, 443, 275-280.

Esmaeilnezhad, E., Choi, H. J., Schaffie, M., Gholizadeh, M., Ranjbar, M., & Kwon, S. H. (2017). Rheological analysis of magnetite added carbonyl iron based magnetorheological fluid. Journal of Magnetism and Magnetic Materials, 444, 161-167.

Genc, S. (2003). Synthesis and Properties of Magnetorheological (MR) Fluids. University of Pittsburgh,

Goldasz, J., & Sapiński, B. (2017). Magnetostatic Analysis of a Pinch Mode Magnetorheological Valve. Acta Mechanica et Automatica, 11. doi:10.1515/ama-2017-0035

Gołdasz, J., & Sapiński, B. (2017). Magnetostatic analysis of a pinch mode magnetorheological valve. Acta Mechanica et Automatica, 11(3), 229-232.

Goncalves, F., & Carlson, J. (2009). An alternate operation mode for MR fluids—magnetic gradient pinch. Journal of Physics: Conference Series, 149, 012050. doi:10.1088/1742-6596/149/1/012050

Goncalves, F., & Carlson, J. (2009). An alternate operation mode for MR fluids—magnetic gradient pinch. Paper presented at the Journal of Physics: Conference Series.

Goncalves, F. D. (2005). Characterizing the Behavior of Magnetorheological Fluids at High Velocities and High Shear Rates. Virginia Tech,

Goncalves, F. D., Ahmadian, M., & Carlson, J. (2005). Investigating the magnetorheological effect at high flow velocities. Smart Materials and Structures, 15(1), 75.

Grunwald, A., & Olabi, A. G. (2008). Design of magneto-rheological (MR) valve. Sensors and Actuators A: Physical, 148(1), 211-223. doi:https://doi.org/10.1016/j.sna.2008.07.028

Horak, W., Sapiński, B., & Szczęch, M. (2017). Analysis of force in MR fluids during oscillatory compression squeeze. Acta Mechanica et Automatica, 11(1), 64-68.

Hu, G., Long, M., Yu, L., & Li, W. (2014). Design and performance evaluation of a novel magnetorheological valve with a tunable resistance gap. Smart Materials and Structures, 23(12), 127001.

Hu, Z., Yan, H., Qiu, H., Zhang, P., & Liu, Q. (2012). Friction and wear of magnetorheological fluid under magnetic field. Wear, 278, 48-52.

Jang, K.-I., Min, B.-K., & Seok, J. (2011). A behavior model of a magnetorheological fluid in direct shear mode. Journal of Magnetism and Magnetic Materials, 323(10), 1324-1329.

Khan, S. A., Suresh, A., & Seetharamaiah, N. (2014). Principles, characteristics and applications of magneto rheological fluid damper in flow and shear mode. Procedia materials science, 6, 1547-1556.

Mazlan, S., Issa, A., Chowdhury, H., & Olabi, A. (2009). Magnetic circuit design for the squeeze mode experiments on magnetorheological fluids. Materials & Design, 30(6), 1985-1993.

Meeker, D. (2010). Finite element method magnetics. FEMM, 4, 32.

Munoz, B. C., Adams, G. W., & Kitchin, J. R. (2001).

Nguyen, Q.-H., & Choi, S.-B. (2012). Optimal Design Methodology of Magnetorheological Fluid Based Mechanisms. In G. Berselli, R. Vertechy, & G. Vassura (Eds.), Smart Actuation and Sensing Systems - Recent Advances and Future Challenges: IntechOpen.

Phule, P. P. (2001). Magnetorheological (MR) fluids: principles and applications. Smart Materials Bulletin, 2001(2), 7-10.

Rosiakowski, A., & Sedziak, D. (2012). Research on clutch with magnetorheological fluid working as a mechanical fuse in a drive-load system. Archives of Mechanical Technology and Automation, 32(4), 23-31.

Rwei, S.-P., Ranganathan, P., Chiang, W.-Y., & Wang, T.-Y. (2017). The magnetorheological fluid of carbonyl iron suspension blended with grafted MWCNT or graphene. Journal of Magnetism and Magnetic Materials, 443, 58-66.

Sarkar, C., & Hirani, H. (2015). Effect of particle size on shear stress of magnetorheological fluids. Smart Science, 3(2), 65-73.

Vékás, L. (2008). Ferrofluids and magnetorheological fluids. Paper presented at the Advances in science and technology.

Wang, G., Zhao, D., Ma, Y., Zhang, Z., Che, H., Mu, J., . . . Dong, X. (2017). Synthesis of calcium ferrite nanocrystal clusters for magnetorheological fluid with enhanced sedimentation stability. Powder Technology, 322, 47-53.

Wang, S. (2011). Control of a uni-axial magnetorheological vibration isolator. University of Toledo,

Wereley, N. M., & Pang, L. (1998). Nondimensional analysis of semi-active electrorheological and magnetorheological dampers using approximate parallel plate models. Smart Materials and Structures, 7(5), 732.

Xu, Z.-D., Guo, W.-Y., & Chen, B.-B. (2014). Preparation, Property Tests, and Limited Chain Model of Magnetorheological Fluid. Journal of Materials in Civil Engineering, 27, 04014229. doi:10.1061/(ASCE)MT.1943-5533.0001190

Yazid, I. I. M., Mazlan, S. A., Kikuchi, T., Zamzuri, H., & Imaduddin, F. (2014). Design of magnetorheological damper with a combination of shear and squeeze modes. Materials & Design (1980-2015), 54, 87-95.

Yoo, J.-H., & Wereley, N. (2002). Design of a High-Efficiency Magnetorheological Valve. Journal of Intelligent Material Systems and Structures - J INTEL MAT SYST STRUCT, 13, 679-685. doi:10.1177/1045389X02013010012

APPENDIX A
PUBLISHED PAPER 1

IOP Publishing   Smart Materials and Structures
Smart Mater. Struct. 26 (2017) 115009 (11pp)   https://doi.org/10.1088/1361-665X/aa8d8f

Thermal conductivity enhancement and sedimentation reduction of magnetorheological fluids with nano-sized Cu and Al additives

M S A Rahim[1], I Ismail[1,2,5], S B Choi[3,5], W H Azmi[2,4] and S N Aqida[4]

[1] Faculty of Manufacturing Engineering, Universiti Malaysia Pahang, 26600 Pekan, Pahang, Malaysia
[2] Automotive Engineering Centre, Universiti Malaysia Pahang, 26600 Pekan, Pahang, Malaysia
[3] Smart Structures and Systems Laboratory, Department of Mechanical Engineering, Inha University, Incheon 402-751, Republic of Korea
[4] Faculty of Mechanical Engineering, Universiti Malaysia Pahang, 26600 Pekan, Pahang, Malaysia

E-mail: izwanismail@ump.edu.my and seungbok@inha.ac.kr

Received 14 June 2017, revised 14 September 2017
Accepted for publication 19 September 2017
Published 4 October 2017

Abstract

This work presents enhanced material characteristics of smart magnetorheological (MR) fluids by utilizing nano-sized metal particles. Especially, enhancement of thermal conductivity and reduction of sedimentation rate of MR fluids those are crucial properties for applications of MR fluids are focussed. In order to achieve this goal, a series of MR fluid samples are prepared using carbonyl iron particles (CIP) and hydraulic oil, and adding nano-sized particles of copper (Cu), aluminium (Al), and fumed silica (SiO_2). Subsequently, the thermal conductivity is measured by the thermal property analyser and the sedimentation of MR fluids is measured using glass tubes without any excitation for a long time. The measured thermal conductivity is then compared with theoretical models such as Maxwell model at various CIP concentrations. In addition, in order to show the effectiveness of MR fluids synthesized in this work, the thermal conductivity of MRF-132DG which is commercially available is measured and compared with those of the prepared samples. It is observed that the thermal conductivity of the samples is much better than MRF-132DG showing the 148% increment with 40 vol% of the magnetic particles. It is also observed that the sedimentation rate of the prepared MR fluid samples is less than that of MRF-132DG showing 9% reduction with 40 vol% of the magnetic particles. The mixture optimized sample with high conductivity and low sedimentation was also obtained. The magnetization of the sample recorded an enhancement of 70.5% when compared to MRF-132DG. Furthermore, the shear yield stress of the sample were also increased with and without the influence of magnetic field.

Keywords: magnetorheological fluid, thermal conductivity, sedimentation rate, copper additive, aluminium additive, nano-sized particle

(Some figures may appear in colour only in the online journal)

1. Introduction

Magnetorheological (MR) fluids are suspensions composed of magnetizable microparticles dispersed in non-magnetic carrier fluids such as hydraulic oil (HO). Since 1995 MR fluids have

[5] Authors to whom any correspondence should be addressed.

thermal conductivity of MRF with the additives will be developed based on the results presented in this work. For further extension, the thermal conductivity of MRF with the additives will be also determined under varied intensity of the magnetic field.

Acknowledgments

The authors are grateful to Universiti Malaysia Pahang (UMP) and Automotive Engineering Centre for financial support given under RDU160132 and RDU160318.

ORCID iDs

M S A Rahim https://orcid.org/0000-0002-4105-6268

References

[1] Imaduddin F, Mazlan S A and Zamzuri H 2013 A design and modelling review of rotary magnetorheological damper *Mater. Des.* **51** 575–91
[2] Qing O, Jiajia Z, Zhaochun L, Ming H and Jiong W 2016 Controllability analysis and testing of a novel magnetorheological absorber for field gun recoil mitigation *Smart Mater. Struct.* **25** 115041
[3] Yaojung S, Nguyen Anh N and Chien-Hung L 2016 Optimal design of a new multipole bilayer magnetorheological brake *Smart Mater. Struct.* **25** 115015
[4] Rizzo R 2017 An innovative multi-gap clutch based on magneto-rheological fluids and electrodynamic effects: magnetic design and experimental characterization *Smart Mater. Struct.* **26** 015007
[5] Ashtiani M, Hashemabadi S and Ghaffari A 2015 A review on the magnetorheological fluid preparation and stabilization *J. Magn. Magn. Mater.* **374** 716–30
[6] Carlson J D and Jolly M R 2000 MR fluid, foam and elastomer devices *Mechatronics* **10** 555–69
[7] Olabi A G and Grunwald A 2007 Design and application of magneto-rheological fluid *Mater. Des.* **28** 2658–64
[8] Yu G, Du C and Sun T 2015 Thermodynamic behaviors of a kind of self-decoupling magnetorheological damper *Shock Vib.* **501** 502747
[9] Patil S R, Powar K P and Sawant S M 2016 Thermal analysis of magnetorheological brake for automotive application *Appl. Therm. Eng.* **98** 238–45
[10] Wang D, Zi B, Zeng Y, Hou Y and Meng Q 2014 Temperature-dependent material properties of the components of magnetorheological fluids *J. Mater. Sci.* **49** 8459–70
[11] Wang D, Zi B, Zeng Y, Xie F and Hou Y 2015 An investigation of thermal characteristics of a liquid-cooled magnetorheological fluid-based clutch *Smart Mater. Struct.* **24** 055020
[12] López-López M T, de Vicente J, González-Caballero F and Durán J D G 2005 Stability of magnetizable colloidal suspensions by addition of oleic acid and silica nanoparticles *Colloids Surf.* A **264** 75–81
[13] Forero-Sandoval I Y, Vega-Flick A, Alvarado-Gil J J and Medina-Esquivel R A 2017 Study of thermal conductivity of magnetorheological fluids using the thermal-wave resonant cavity and its relationship with the viscosity *Smart Mater. Struct.* **26** 025010
[14] Yildirim G and Genc S 2013 Experimental study on heat transfer of the magnetorheological fluids *Smart Mater. Struct.* **22** 1–8
[15] Shulman Z P, Kordonsky V I and Demchuk S A 1979 The mechanism of heat transfer in magnetorheological systems *Int. J. Heat Mass Transfer* **22** 389–94
[16] Li Q, Xuan Y and Wang J 2005 Experimental investigations on transport properties of magnetic fluids *Exp. Therm. Fluid Sci.* **30** 109–16
[17] Sharif M Z, Azmi W H, Redhwan A A M and Mamat R 2016 Investigation of thermal conductivity and viscosity of Al_2O_3/PAG nanolubricant for application in automotive air conditioning system *Int. J. Refrig.* **70** 93–102
[18] Chon C H, Kihm K D, Lee S P and Choi S U S 2005 Empirical correlation finding the role of temperature and particle size for nanofluid (Al_2O_3) thermal conductivity enhancement *Appl. Phys. Lett.* **87** 1531071–3
[19] Patel H, Sundararajan T and Das S 2010 An experimental investigation into the thermal conductivity enhancement in oxide and metallic nanofluids *J. Nanopart. Res.* **12** 1015–31
[20] Eastman J A, Choi S U S, Li S, Yu W and Thompson L J 2001 Anomalously increased effective thermal conductivities of ethylene glycol-based nanofluids containing copper nanoparticles *Appl. Phys. Lett.* **78** 718–20
[21] Jana S, Salehi-Khojin A and Zhong W-H 2007 Enhancement of fluid thermal conductivity by the addition of single and hybrid nano-additives *Thermochim. Acta* **462** 45–55
[22] Mrlík M, Ilčíková M, Pavlínek V, Mosnáček J, Peer P and Filip P 2013 Improved thermooxidation and sedimentation stability of covalently-coated carbonyl iron particles with cholesteryl groups and their influence on magnetorheology *J. Colloid Interface Sci.* **396** 146–51
[23] Lim S T, Cho M S, Jang I B and Choi H J 2004 Magnetorheological characterization of carbonyl iron based suspension stabilized by fumed silica *J. Magn. Magn. Mater.* **282** 170–3
[24] Triefenbach F 2008 *Design of Experiments: The D-Optimal Approach and its Implementation as a Computer Algorithm* (Meschede: South Westphalia University of Applied Sciences)
[25] Alves S, Alcantara M R and Figueiredo Neto A M 2009 The effect of hydrophobic and hydrophilic fumed silica on the rheology of magnetorheological suspensions *J. Rheol.* **53** 651–62
[26] Yang J, Yan H, Hu Z and Ding D 2016 Viscosity and sedimentation behaviors of the magnetorheological suspensions with oleic acid/dimer acid as surfactants *J. Magn. Magn. Mater.* **417** 214–21
[27] Maxwell J C 1904 *A Treatise on Electricity and Magnetism* (Cambridge, UK: Oxford University Press)
[28] Reinecke B N, Shan J W, Suabedissen K K and Cherkasova A S 2008 On the anisotropic thermal conductivity of magnetorheological suspensions *J. Appl. Phys.* **104** 1–7
[29] Bruggeman D 1935 The prediction of the thermal conductivity of heterogeneous mixtures *Ann. Phys.* **24** 636–64
[30] Xie H, Wang J, Xi T, Liu Y, Ai F and Wu Q 2002 Thermal conductivity enhancement of suspensions containing nanosized alumina particles *J. Appl. Phys.* **91** 4568–72
[31] Murshed S S, Leong K C and Yang C 2010 *Handbook of Nanophysics: Nanoparticles and Quantum Dots* vol 3 ed K D Sattler (Florida: CRC Press) pp 1–14
[32] Rahim M S A, Ismail I and Aqida S N 2017 Effects of nano copper additive on thermal conductivity of magnetorheological fluid at different environment temperature *Mater. Sci. Forum* **890** 108–11

APPENDIX B
PUBLISHED PAPER 2

Materials Science Forum
ISSN: 1662-9752, Vol. 890, pp 108-111
doi:10.4028/www.scientific.net/MSF.890.108

Submitted: 2016-11-14
Accepted: 2016-11-17
Online: 2017-03-20

Effects of Nano Copper Additive on Thermal Conductivity of Magnetorheological Fluid at Different Environment Temperature

MOHD Salleh Abdul Rahim[1,a*], IZWAN Ismail[1,2,b] and SYARIFAH Nur Aqida[3,c]

[1]Faculty of Manufacturing Engineering, Universiti Malaysia Pahang, 26600 Pekan, Malaysia.

[2]Automotive Engineering Centre, Universiti Malaysia Pahang, 26600 Pekan, Malaysia.

[3]Faculty of Mechanical Engineering, Universiti Malaysia Pahang, 26600 Pekan, Malaysia.

[a]sallehrahim@icloud.com, [b]izwanismail@ump.edu.my, [c]aqida@ump.edu.my

Keywords: Magnetorheological fluid; thermal conductivity; high temperature; nano copper.

Abstract. Low thermal conductivity of magnetorheological (MR) fluid limits its potential to be applied in high temperature environment. Recently, enhancing thermal conductivity of similar fluids through addition of nano copper has attracted to address the problem. This paper presents the effects of nano copper addition on thermal conductivity properties of MR fluid at different environment temperatures. The nano copper added MR fluid samples were synthesized with carbonyl iron powder in hydraulic oil. The samples were then stabilized with addition of fumed silica and were homogenized using ultrasonic bath. Thermal conductivity of the samples and references material was measured using thermal property analyser. The environment temperature of the samples was controlled by waterbath incubation method. The results showed that enhancement of thermal conductivity with the presence of copper nanoparticles was higher at 40 vol% of CIP compared to 20 vol% of CIP and a slight variation in thermal conductivity of MR fluid was observed in environment temperatures of 30–70°C. This finding leads to development of new class of magnetorheological fluid with enhanced thermal properties.

Introduction

Magnetorheological (MR) fluids possess phase change behaviour where rheological properties of the material are alterable with magnetic field [1]. Due to this advantage, MR fluid is beneficial to be applied in active and semi-active devices [2]. However, at high temperature environment, instability behaviour of shear thinning and decreasing shear stress is significant. Improving thermal conductivity of MR fluid may dissipate heat at higher rate and eventually overcome those problems.

Analogous to materials like ferrofluids, thermal conductivity of MR fluid can be increased by either increasing particle volume fraction of magnetic particles [3, 4] or adding nano-metal particle [5, 6]. Smaller particles size resulted in increment of thermal conductivity as much as 5% in Al2O3 nanofluid with 150 nm particles size. Whereas, in nanofluid containing 47 nm particles size, 10% enhancement of thermal conductivity was recorded [7]. Furthermore, base fluid properties are significant to set minimum value of thermal conductivity. In a study of base fluids effect on thermal conductivity of nanofluid containing graphene oxide nanosheets, mineral oil based fluid was found to enhance the thermal conductivity by ratio of 76.8% compared to propylene glycol at 62.3% and distilled water at 30.2% [8]. Enhancement of thermal conductivity was also reported in metals and metal-oxide based nanofluids where aluminium and alumina additive enhanced thermal conductivity by 27% and 17%, respectively [8]. Copper nanoparticle has been reported as an additive in nanofluids with high melting point temperature, non-magnetic and high thermal conductivity [9]. In this study, the effect of copper nanoparticle additive in MR fluids was measured. MR fluid samples were measured at different CIP, base fluid, and copper nanoparticles percentages.

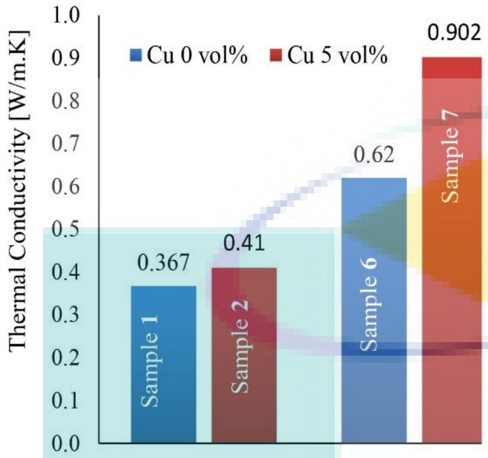

Figure 2. Effect of copper nanoparticles additive on thermal conductivity.

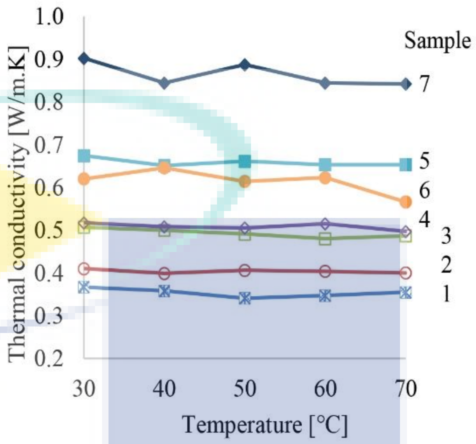

Figure 3. Effect of temperature to thermal conductivity.

Conclusion

Thermal conductivity of MR fluids with addition of copper nanoparticles was enhanced. At 40 volume % of CIP, increased of thermal conductivity was higher than MR fluid sample of 20 volume % of CIP. The changes of environment temperatures from 30 to 70°C were unable to vary the thermal conductivity of MR fluids with standard deviations of less than 0.03 W/m.K.

Acknowledgement

This work was financially supported by University Malaysia Pahang (Grant No. RDU160318).

References

[1] S.E. Premalatha, R. Chokkalingam and M. Mahendran: Am. J. Polym. Sci. Vol. 2(4) (2012), p. 50-55

[2] I. Ismail, S.A. Mazlan, H. Zamzuri and A.G. Olabi: Jpn. J Appl. Phys. Vol. 51 (2012), p. 067301

[3] H. Cheng, W. Hong and C. Liu: J. Chinese Adv. Mater. Soc. Vol 2 (2014), p. 130-137

[4] M.S.A Rahim and I. Ismail: IOP Conf. Ser. Mater. Sci. Eng. Vol 100 (2015), p. 012040

[5] H. Patel, T. Sundararajan and S. Das: J. Nanopart. Res. Vol 12 (2010), p. 1015-1031

[6] M. Lomascolo, G. Colangelo, M. Milanese and A. de Risi: Renew. Sustainable Energy Rev. Vol. 43 (2015), p. 1182-1198

[7] C.H. Chon, K.D. Kihm, S.P. Lee and S.U. Choi: Appl. Phy. Lett. Vol. 87 (2005), p. 153107

[8] W. Yu, H. Xie and W. Chen: J. Appl. Phy. Vol. 107 (2010), p. 094317

[9] A. Tamilvanan, K. Balamurugan, K. Ponappa and B.M. Kumar: Int. J. Nanosci. Vol. 13 (2014), p. 1430001

[10] S. Wahid, I. Ismail I, S. Aid and M.S.A. Rahim: IOP Conf. Ser. Mater. Sci. Eng. Vol. 114 (2016), p. 012101

[11] C. Sarkar and H. Hirani: Tribology Online Vol. 10 (2015), p. 282-294